

Modeling and Optimization of Nanofluid Based Heat Exchanger using ANN

A Dissertation submitted
in partial fulfilment of the requirements
for the award of degree of

Master of Engineering

in

Thermal Engineering

by

Navneet Arya

Registration No.: 801483016

Under the Supervision of

MR. Kundan Lal

(Assistant Professor)

DR. V. K. Sangal

(Associate Professor)



**DEPARTMENT OF MECHANICAL ENGINEERING
THAPAR UNIVERSITY, PATIALA**

July, 2016

CERTIFICATE

I hereby declare that the thesis entitled “**Modeling and Optimization of Nano Fluid Based Heat Exchanger using ANN**” is an authentic record of my work carried out as requirements for the award of the degree of **Master of Engineering in Thermal Engineering** at **Thapar University, Patiala** under the supervision of **Dr. V. K. Sangal**, Associate Professor, Chemical Engineering Department, Thapar University, Patiala and **Mr. Kundan Lal**, Assistant Professor, Mechanical Engineering Department, Thapar University, Patiala during July, 2014 to July, 2016. No part of the matter embodied in this report has been submitted to any other university or institute for the award of any degree.

Date: 15/7/16

Navneet
Navneet Arya

It is certified that the above statement made by the student is correct to the best of my/our knowledge and belief.

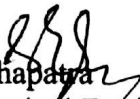


Mr. Kundan Lal
Assistant Professor, MED
Thapar University, Patiala-147004



Dr. V. K. Sangal
Associate Professor, Chemical Engineering
Thapar University, Patiala-147004

Countersigned by



Dr. S.K. Mohapatra
Head, Mechanical Engineering Department
Thapar University, Patiala-147004



Dr. S.S. Bhatia
Dean of Academic Affairs
Thapar University, Patiala-147004

Dedication

I dedicate this thesis to my beloved father Bhagi Rath Arya and my mother Lakshmi Arya, who are an ever supporting and encouraging with their great patience. I also dedicate this to my sister Nitika Arya, who stood as an impression and to all my dearest friends.

ACKNOWLEDGEMENT

Words are less to reveals one's deep regard. I would like to express my sincere of gratitude and respect to all of those who help me out during my thesis work.

This work have been possible due to guidance and encouragement of my supervisor Dr. V. K. Sangal and Mr. Kundan Lal. There guidance and immense knowledge helped me to complete this thesis work. This thesis work are result of numerous of our discussions. There feedback and guidance are invaluable to complete this work.

I am thankful to Thaper University Patiala for providing me such a great atmosphere and exposure.

I would also thankful to all the researcher whose precious work help me for this thesis work. Last but not least, I would like to thank my parents for their unconditional love and support.

Navneet
Navneet Arya

Abstract

In the present study the heat transfer coefficient and friction factor is simulate by the artificial neural feed forward network for double tube heat exchanger using TiO₂-water nanofluid with twisted tape. The back propagation learning algorithm is used by ANN model. The developed ANN model for heat transfer coefficient have regression coefficient of 0.9974. Heat transfer coefficient and friction factor are experimentally investigated in a turbulent flow regime. The volume concentration of TiO₂-water nanofluid is 0.01%, 0.025% and 0.05% and twisted tape ratio 3.5, 4.6 and 6.5 respectively. The mass flow rate of hot side fluid ranges from 0.0163-0.0816 Kg/s and cold side flow rate is fixed to 4LPM. The experiments were conducted both water and TiO₂-water nanofluid. The result shows that the Dittus-Bolter predicted Nusselt number with good agreement with experiment for plain tube. The Nusselt number enhances with Reynold number for plain tube. The heat transfer coefficient for twisted tape increases with decrease in twisted tape that is due to the increase in residence time, swirl flow and better fluid mixing. The heat transfer coefficient enhances 53.4%, 47.9% and 34.4% with twisted tape ratio 3.5, 4.6 and 6.5 compared to plain tube. Furthermore with increase in concentration TiO₂-water the maximum heat transfer coefficient enhance 3.17% with 0.05% TiO₂-water the compared to water. The use of these enhancement techniques effects the friction factor too. The predicted friction by Blasius have good agreement with the experimental data. The developed ANN model for friction factor have regression coefficient of 0.9902. The friction factor decrease with increase in Reynold number. The use of twisted tape led to enhancement in friction factor as well. The results show that as twisted tape ratio decrease the friction factor enhances. The twisted tape ratio 3.5 provides highest friction factor 1.96 times compared to water in plain tube. The twisted tape insert with TiO₂-water nanofluid provides the highest friction factor and heat transfer coefficient which is about 1.96 times and 53.4% compared to plain tube with water as fluid. The ANN predicts the result accurately compared to the correlation used to validate the tube and twisted tape. The predicted heat transfer coefficient and friction factor by ANN developed model are found to be in good agreement with experimental data.

Keywords: Double tube heat exchanger, Nanoparticles, Artificial Neural Network, Twisted tape, Heat transfer coefficient, Friction factor.

Table of Content

	Page No.
THESIS CERTIFICATION	i
DEDICATION	ii
ACKNOWLEDGEMENT	iii
ABSTRACT	iv
TABLE OF CONTENTS	v
LIST OF FIGURES	viii
LIST OF TABLES	x
NOMENLATURE	xi
Chapter 1	
Introduction	
1.1 Introduction to heat exchanger	1
1.2 Need for enhancement of heat transfer in heat exchangers	1
1.3 Introduction to nanofluids	2
1.4 Nano materials and basefluid	2
1.5 Heat transfer enhancement techniques	3
1.6 Nano particles in suspension	3
1.7 Preparation method for nanofluids	4
1.8 Feature of nanofluids	5
1.9 Artificial Neural Network	5
2.0 Application of Artificial Neural Network	7
Chapter 2	
Literature Review	
2.1 Swirl Flow Devices	9

2.2	Liquid Additives	12
2.3	Combination of Swirl Flow devices and Additives	16

Chapter 3

Research Gaps and objectives

3.1	Research Gaps	25
3.2	Research Objectives	26

Chapter 4

Experimental Setup and Methodology

4.1	Experimental setup	27
4.2	Twisted tape inserts	30
4.3	Nanofluid	31
4.3.1	Estimation of amount of Nanoparticles	31
4.3.2	Preparation of Nanofluid	31
4.3.3	Mixing of TiO ₂ -nanoparticles in water	32
4.3.4	Adding surfactants to water	32
4.3.5	Determination of properties of TiO ₂ nanofluid	33
4.4	Experimental Procedure	35
4.5	Artificial Neural Network Modeling	36
4.5	Varied parameter in experimental study	37
4.6	Precaution	37

Chapter 5

Results and Discussion

5.1	Heat Transfer Coefficient	38
-----	---------------------------	----

5.1.1	Development of ANN model	38
5.1.2	Validation of Plain Tube	40
5.1.3	Effect of Twisted Tape inserts on Nusselt number	42
5.1.4.	Plain Tube with TiO ₂ -water nanofluid	44
5.1.5	Effect of TiO ₂ -water nanofluid with the Twisted Tape	45
5.1.6	Effect of Plain tube, TiO ₂ -water nanofluid, Twisted Tape with and without TiO ₂ -water nanofluid on heat transfer coefficient	48
5.2	Friction Factor	49
5.2.1	Development of ANN model for friction factor	49
5.2.2	Validation of Plain Tube	52
5.2.3	Effect of Twisted Tape inserts on friction factor	54
5.2.4	Plain Tube with TiO ₂ -water nanofluid	56
5.2.5	Effect of TiO ₂ -waer nanofluid with the Twisted Tape on the friction factor	56
5.2.6	Effect of Plain tube, TiO ₂ -water nanofluid, Twisted Tape with and without TiO ₂ -water nanofluid on the friction factor	59

Chapter 6

Conclusions and Future scope

6.1	Conclusions	61
6.2	Future Scope	62

Reference	63
------------------	----

Appendix	68
-----------------	----

List of Figures

		Page No.
Figure 4.1	Pictorial view of counter flow heat exchanger	28
Figure 4.2	Pictorial view of PID	28
Figure 4.3	Pictorial view of Temperature displayer	29
Figure 4.4	Pictorial view of pump	29
Figure 4.5	Pictorial view of twisted tape	30
Figure 4.6	Pictorial view of TiO ₂ nanoparticles	31
Figure 4.7	Pictorial view of magnetic stirrer and ultrasonic bath	32
Figure 4.8	Pictorial view of TiO ₂ nanofluid	32
Figure 4.9	Pictorial view of KD2 Pro	33
Figure 4.10	Pictorial view of Brookfield viscometer	34
Figure 4.11	Experimental setup layout	34
Figure 4.12	Pictorial view of experimental setup	35
Figure 5.1	Feed Forward back propagation ANN model	38
Figure 5.2(a)	Regression plot for ANN Model for heat transfer coefficient	39
Figure 5.2(b)	Effect of hidden layer number of neuron of ANN model performance	40
Figure 5.3	Validation of Nusselt number of Plain Tube with the Dittus Bolter	41
Figure 5.4	Comparison of ANN model with the experimental data	42
Figure 5.5	Validation of Nusselt number of Twisted Tape with Manglik and Bergies	43
Figure 5.6	ANN model used to predict the heat transfer coefficient of twisted tape	44
Figure 5.7	variation of heat transfer coefficient with TiO ₂ concentration	45
Figure 5.8	Variation of heat transfer coefficient with twisted tape ratio (H/D=3.5, 4.6 and 6.5) at 0.01% concentration of TiO ₂ -water	46

Figure 5.9	Variation of heat transfer coefficient with twisted tape ratio (H/D=3.5, 4.6 and 6.5) at 0.025% concentration of TiO ₂ -water	47
Figure 5.10	Variation of heat transfer coefficient with twisted tape ratio (H/D=3.5, 4.6 and 6.5) at 0.05% concentration of TiO ₂ -water	48
Figure 5.11	Comparison of different heat transfer coefficient techniques with the plain tube	49
Figure 5.12	Feed forward back propagation neural network	50
Figure 5.13.a	Regression plot for ANN model for friction factor	51
Figure 5.13.b	Effect of hidden layer number of neuron of ANN model performance	52
Figure 5.14	Validation of friction factor of Plain Tube with the Blasius equation	53
Figure 5.15	Comparison of friction factor of Plain Tube with the ANN model	54
Figure 5.16	Variation of friction factor with the twisted tape ratio	55
Figure 5.17	Variation of friction factor with the TiO ₂ -water	56
Figure 5.18	Variation of friction factor with the twisted tape ratio (H/D=3.5, 4.6 and 6.5) at 0.01% TiO ₂ -water concentration	57
Figure 5.19	Variation of friction factor with the twisted tape ratio (H/D=3.5, 4.6 and 6.5) at 0.025% TiO ₂ -water concentration	58
Figure 5.20	Variation of friction factor with the twisted tape ratio (H/D=3.5, 4.6 and 6.5) at 0.05% TiO ₂ -water concentration	59
Figure 5.21	Comparison of effect of different heat transfer coefficient enhancement technique on friction factor	60

List of Table

		Page No.
Table 4.1	Volume concentration of TiO ₂ with corresponding weight	31

LIST OF SYMBOLS AND ABBREVIATIONS

Nomenclature

A	Cross section area, m^2
D_h	Hydraulic diameter, m
D_p	Nanoparticle diameter, m
F	Darcy friction factor
H	Average Heat Transfer Coefficient $W/m K$
Δp	Pressure Drop
Re	Reynold number
K	Thermal Conductivity, $W/m.k$
C_p	Specific heat , $Kj/Kg K$
Nu	Nusselt number
T	Temperature
Q	Heat input , W
V	Volume, L

Greek symbols

Δ	Thickness of strip, m
α	Thermal diffusivity, m^2/s
\varnothing	Volume concentration , %
μ	Absolute viscosity, $Kg/m s$

P Density. Kg/m³

n_b Base fluid

Acronym

MAE Mean Absolute Error

MLFFN Multi-Layer Feed Forward Network

RMS Root Mean Square

MRE Mean Relative Error

MSE Mean Square Error

Chapter 1

Introduction

1.1 Introduction to heat exchanger

Heat exchangers are device that provide the flow of thermal energy between two or more fluids maintained at different temperatures. The flow may be separated by a solid wall to prevent mixing or they may be in direct contact. The heat exchangers have wide range of applications such as; in power production, chemical processes, food industries, electronics environmental engineering, air conditioning, waste heat recovery and the space applications .

Heat exchanger are classified according to following criteria

- 1 Regenerators
- 2 Transfer processes direct and indirect contact.
- 3 Geometry of construction tubes, plates and extended surface.
- 4 Heat transfer mechanisms single phase and two phases.
- 5 Flow arrangement, parallel, counter and cross flow.

Common applications of heat exchangers

- Cooling of vehicles with the help of radiator
- Condensers and evaporators of air conditioning systems
- Space heating

1.2 Need for enhancement of heat transfer in heat exchangers

The thermal performance of a heat exchanger depends upon many factors such as; geometry of heat exchanger, its kinetic and spatial aspects, related to net heat transfer rate encountered between the heat transfer sections and fluid and flow properties. To enhance the heat transfer rate of a heat exchanger, there are active and passive methods. The active method is related with the fluid and the passive method is related to the heat exchanger. The active method includes to create the turbulence in the fluid flow, using the fluid with higher thermophysical properties. The thermophysical properties include the thermal conductivity, dynamic viscosity; density and specific heat. The passive method include the type of tube, number of tubes, tubes pitch, layout angle and length. In addition to the main factors, other

parameters which also effect the thermal performance of heat exchanger are fouling factor, pressure drop and pumping power. The decrease in the values of these factors will lead to higher performance of the heat exchanger. The heat transfer enhancement is done to save the energy and to reduce the process time. In industries, the heat exchangers with minimal surface area are required. For the optimal conversion, the systems are required to be designed for the highest efficiency at low cost. The heat transfer enhancement increase the performance of heat exchanger and efficiency of heat exchange between the working fluids.

1.3 Introduction to nanofluids

The modern technology is able to produce the nano-size particles which have thermal, optical, chemical properties different from the parent materials. The use of these nano-size particles in basefluid lead to introduce in thermo physical properties. The enhancement in the thermos-physical properties effect the thermal performance of the heat exchangers.

The nanofluids are prepared by the suspending the nanoparticles suspended in the basefluids. The base fluid may be water, ethylene glycol, oil, hydrocarbon, flu carbon etc. Nanoparticles are the particles which have its one dimension in nano scale means 1-100 nm. The nanofluids have more effect on the thermal performance compared to as that of basefluid. The nanofluid improve the thermophysical properties of the fluid which help to enhance the thermal performance of heat exchangers. This is due to fact that the thermal conductivity of solid is more than the liquid or gases fluid. When these solid nanoparticles are dispersed in fluids they result into their higher thermal characteristics. Different nanoparticles material such as oxides, metal, nitrides, non-metals. The nanofluid are more costlier than the microfluid. But we are using the nanofluid instead of micro fluid due to the properties of nano fluid like the aspect ratio which is about 1000 times the micro particles and the other is that it clog the heat exchanger tube .The other factor is that the nanoparticle suspended in the fluid more better than the micro fluid. The objective of using nanofluid is to achieve the improved thermal properties by adding small amount of nanoparticle in nanofluid.

1.4 Nano materials and basefluid

Nano particles materials are;

- Metal AL, Cu
- Metal carbides Sic

- Nitrides SiN
- Non-metals graphite, carbon nano tubes
- Oxides ceramics

Basefluid include are as follow;

- Water
- Ethylene Glycol
- Oil
- Hydrocarbon

1.5 Heat transfer enhancement techniques

To increase the thermal performance of the heat exchangers three different techniques are followed discussed below:

Passive techniques: In passive technique the heat transfer enhancement is generally augment with the geometrical and surface modifications to flow passage by implementing inserts or additional devices. Examples of such technique are inserts, coiled tubes, surface tension devices, swirl flow devices, treated surface and fluids additives [Liebenberg and Meyer, 2007].

Active techniques: In active techniques, the enhancement is achieved by some external power inputs. Some of active techniques such as; mechanical aids, surface vibration, suction or injection, jet impingement, fluid vibration. The main disadvantage of active techniques is required some external power sources. So they have limited application in comparison to other techniques [Elshafei et al., 2008].

Compound techniques: In compound techniques the heat transfer is enhanced by combination of above explained two techniques [Alamgholilou and Esmaeilzadeh, 2012].

1.6 Nano particles in suspension

The suspension of nanoparticle in basefluid is influenced by the following factor;

1.6.1 Cohesive tendency

These depend upon the particles characteristics

- Hydro phobic particles attract in water.

- Hydrophilic particles repel in water.
- Surfactant coating of nano particles in suspension help to keep them apart.

Cohesive forces as a function of inter particle distance in colloidal suspension. The dilute suspended particles have less chance of avoiding cohesion are better. But as the particles concentration increase and inter particles distance decrease the force of adhesion between the particles become much larger

Cohesive forces

$$F_{\text{coh}} = F_{\text{vdw}} + F_{\text{es}} + F_{\text{capillary}} + F_{\text{viscous}} + F_{\text{contact}}$$

$$F_{\text{vdw}} = A_{\text{rp}}/12s^2$$

$$F_{\text{es}} = Q_1 Q_2 / 4\pi \epsilon_r \epsilon_0 S^2$$

$$F_{\text{capillary}} = F_{\text{surface tension}} + F_{\text{pressure}}$$

1.6.2 Dynamic behaviour

- Mean size increase with time due to agglomerate
- Total number of particles will decrease with time.
- Population balance modelling required.

Dispersion is generally required. The nanoparticles have tendency to agglomerate to disperse nano particles the following method are used

- Stirring
- Orbital shaking
- Sonification

1.7 Preparation method for nanofluids

Stable suspension particles are provided by two methods:

1.7.1 One step technique:

In this technique the making of nanoparticles and disperse simultaneously into the fluid .In this method the chances of agglomerate are reduced by avoiding the storage, transportation and dispersion of nanoparticles and stability of fluids is increased. One step chemical method is developing in rapidly rather than the one step physical method.

1.7.2 Two-step technique:

In this technique the nanoparticles are created by mechanical comminuting followed by the chemical reaction, vapour condensation. The second step involves to disperse the prepared nanoparticles in base fluid. This technique is applicable for the oxides nano particles and carbon nanotubes are prepared by two step method. Dispersion of nanoparticles are still challenge due to the particles agglomerates rapidly before dispersion and settle down in liquid.

This technique is economic for production of large scale nanoparticles. In this technique the particles are not completely detached and the dispersion of the particles are moderately dispersed. For reducing the chance of overheating of nano particles they are ultrasonically dispersed in liquid.

1.8 Feature of nanofluids

When the nanoparticles are dispersed in the basefluid, the prepared nanofluid have the following features:

- Higher heat conduction: The surface area of nanoparticles is larger so there is more heat transfer in nanofluids. Another feature like the stability of dispersion, attributable to tiny size, which lead to micro convection of fluid and increase heat transfer.
- Stability : The particles are small so the weight of nano particles are also small due to they are easily floating on the base fluid and chance of agglomeration are reduced .This reduction agglomeration lead to eliminate the major drawback settle of particles and make nanofluid more stables.
- Micro channel cooling without clogging: The use of micro particles lead to clog the micro channel for the better conduction fluid and large heat transfer area.
- Reduction the chance of erosion: Due to the nanosize the momentum is also smaller which is impart on the solid wall and less chance of erosion of component such as pump, heat exchanger.

1.9 Artificial Neural Network (ANN)

In the last few years, artificial neural networks (ANNs) have come out as an appealing tools for nonlinear process modeling, particularly in the situations where the improvement of conventional regression models becomes unfeasible. ANN is a computer based model that

solves system through iterations without requiring earlier information of the relationships of process parameters. It is also capable of dealing with uncertainties, noisy data, and non-linear relationships. There are various advantages of an ANN based model including: (1) ANN can be buildup exclusively from the historic process input-output data, (2) detailed information of the process phenomenology is needless for the model development, (3) a properly trained model possesses an exceptional simplification capability owing to which it can exactly predict outputs for a new input data. Owing to their numerous attractive characteristics, ANNs have been extensively used in engineering applications such as steady state and dynamic process modeling, process identification and yield maximization etc.

ANNs are simulated by biological neural systems. Neurons are the basic component of ANN. Two types of ANNs are mostly used as multilayered feed forward neural network, which is trained by back-propagation algorithm and Kohonen self-organizing mapping . Back-propagation algorithm in ANN was used for learning the appropriate weights. The input layer act as receiver and shows the number of input variables used and output layer provide the response which shows the number of result variables whose value is to be predicted. The hidden layers act as feature detectors layers which are employed to perform nonlinear transformations on the input space and are mostly used for computation purposes. More than one hidden layer could be present. According to the theory of universal approximation a network having a single hidden layer and amply large number of neurons could be used to interpret any structure of input and output.

ANN methodology can be broadly divide into three major steps as discussed below

- Selection of ANN parameters
- Training of ANN
- Testing of network

1.9.1 Selection of ANN

Selection of ANN parameter is the first step for ANN modeling. The number of neuron in each layer are different, like in the input layer the number of neuron are depend upon the parameter which affect the performance of heat exchanger. But in hidden layer the number of neuron and number of layer are depend on the required accuracy .The number of

neuron and hidden layer learning rate should be selected optimized so the required accuracy is maintained.

1.9.2 Training of ANN

ANN training with known input output data set and by adjusting the value of weight coefficient between the processing neurons. The error between the output and the desired output has been changed by changing the weights and biases. When the error fall below the determined value the process is terminate automatically.

Step involving for training the ANN are as follows:

- Determine the parameter, which effects the performance of heat exchanger and taken as neuron in the input layer.
- For second law analysis of heat exchanger, the influence of dead state should be considered.
- The data from the experiment are use to train the neural network. The data from the experiment are divided into three data set.
- Normalization of input layer and output layer has been done by the range between 0 and 1. By normalization the speed of training is enhanced.
- For the given Problem the neural network architecture is selected.
- The ANN is trained by the input and output which are taken from the experimental data using the MATLAB.
- The parameter like number of Neuron and number of layer in hidden layer should be optimized to obtain good accuracy.
- Extracting the result from the training network.

1.9.3 Testing of network

Following statistical parameter are used to check the performance of network

- Absolute fraction variance
- Correlation coefficient
- Root mean square value
- Mean absolute relative error

2.0 Application of Artificial Neural Network

2.0.1 ANN modelling of heat exchanger

- Modelling of condensers [Tian et al., 2006]
- Modelling of liquid line suction heat exchanger and evaporators. [Kumlutas et al., 2007]
- Modelling of run around heat exchangers [Akbari et al., 2005]
- Modelling of compact heat exchanger [Tan et al., 2010]
- Modelling of plate type heat exchanger.[peng and ling, 2008]
- Modelling of fin and tube heat exchangers. [Vega et al., 2009]
- Modelling of shell and tube heat exchanger [xie et al., 2005]

2.0.2 Estimate of heat exchanger parameters

- Estimation of heat transfer coefficient
- Estimation of fouling factor
- Estimation of friction factors

2.0.3 Phase change characteristics in heat exchanger

- Boiling characteristics.
- Critical heat flux.
- Estimation of void fraction
- Condensation characteristics

Chapter 2

Literature Review

The purpose of this section is to review the initial study conducted over the previous years related to effect on heat transfer coefficient and friction of TiO₂-water nanofluid with twisted tape inserts in heat exchanger. The reported studies are found to be on the different heat transfer enhancement techniques. In order to improve the thermal performance of heat exchanger three main techniques are used such as; passive, active and compound enhancement technique. Afterward the review was related to the modelling of heat exchanger using artificial neural network. Every conscious effort are made to present the literature review more confined way on heat exchanger enhancement thermal performance techniques and artificial neural network modelling for heat exchanger.

2.1 Swirl Flow Devices

The swirl flow devices causes swirl flow or axial flow secondary recirculation inside a flow channel. Tube inserts include helical strips, twisted tape inserts or cored screw, modified geometry include helically twisted tube, ribs and dimples. These swirl flow devices can be used in both single and double phase heat exchanger. Twisted tape inserts are most commonly used compared to other swirl flow devices due to advantage of easy manufacturing and implementation [Agarwal and Rao, 1996]. The twisted tape insert was used in both the flow region laminar as well as turbulent. But the attention is more toward turbulent flow due to its application in industries and high rate of heat convection coefficient than laminar. So main focus on the turbulent flow region.

Naphon (2006) investigated the heat transfer and pressure drop in a double tube heat exchanger with twisted tape insert. The twisted tape ratio 2.5 and 3.0 was inserted in inner tube of a double tube heat exchanger. A uniform heat flux condition was achieved using the heater and temperature controller. The hot water, cold water and the wall temperature were measured by thermocouple. The pressure drop were measured by digital manometer with accuracy of 0.015%. The Reynold number were varied in range of 5000-30000 for inner tube. Their result showed that the heat transfer rate increased with Reynold number and lower

twisted tape ratio. The friction factor decrease with the Reynold number and higher for twisted tape insert compared to plain tube.

Piriyarungrod et al. (2015) studied the heat transfer rate and friction factor in a tube with tapered twisted tape insert. Twisted tape of different twist ratio, $y/w = 3.5, 4.0$ and 4.5 were used in this study to introduce the swirl flow in tube. The experimental result showed that the heat transfer rate of twisted tape insert was found better than the plain tube. It was found that the use of twisted tape with lower twist ratio in tube results in increase in heat transfer coefficient and friction factor. The mean Nusselt number was found to decrease 10.98% and 6.08% with 4.5 twisted tape ratio compared to the 3.5 and 4.0 twisted tape ratio. Furthermore, they observed that the mean friction factor for twisted tape ratio 4.5 was founded 15.70% and 6.22% less than the twisted ratio of 3.5 and 4.0 respectively.

Eiansa-ard et al. (2008) studied that the heat transfer and friction characteristic in which louvered strip. It was inserted in a concentric double tube heat exchanger under a constant wall heat flux. Louvered strip of different inclined angle ($\theta=15^\circ, 25^\circ$ and 30°) with forward and backward arrangement were used in this study. In their experimental the hot fluid was flowed through inner pipe with varied Reynold number from 6000 to 42000 , cold fluid was flowed in annulus section with constant flow rate. The result showed that the heat transfer and friction factor varied with the strip inclined angle and Reynold number. The higher heat transfer was observed for backward louvered at highest inclination angle. The backward louvered strip showed increase in heat transfer rate 150% to 284% and backward louvered strip shows 133% and 264% compared to the plan tube. It was observed that the friction factor for forward arrangement showed 280% and 413% increase compared to plain tube and showed 155% to 233% for backward louvered strip.

Eiansa ard et al. (2006) investigated the heat transfer and flow friction in a horizontal double pipe heat exchanger fitted with regular spaced twisted tape and full-length twisted tape. Experiments were conducted by varied the Reynold number ($2000-12000$), twisted tape ratio and twisted space. The twisted tape twisted ratio was varied ($y=6.0, 8.0$) and the free space ratio ($S=1, 2$ and 3) were used. The experimental result showed that the mean Nusselt number increase 179% , 160% and 121% compared to the plain tube. It was found that the friction factor decrease with increase in Reynold number. The friction factor decrease 15% , 39% and 81% with increase in twisted space ratio as compared to full- length twisted tape.

Naphon (2006) studied the heat transfer and pressure drop in horizontal concentric tube heat exchanger with coiled wire for turbulent flow. The temperature of cold water and hot water were varied between 15-20°C and 40-45°C. The coiled wire were inserted in the inner tube with varied mass flow rate 0.04 and 0.08 kg/s. The experimental data showed that the heat transfer rate depend upon the mass flow rate of cold and hot water. They observed that the heat transfer rate was enhanced by lower pitch of coil-wire inserts.

Promvonge (2015) studied the influence of V-fins and quadruple counter-twisted tapes on heat transfer and friction factor under the turbulent flow in a square duct. The test were undertaken on air as a fluid with varied Reynold number from 4000 to 30,000. In the experiments were used by varying their parameter such as; relative height ($R_b=0.16, 0.21, 0.32$ and 0.42) and relative pitch ($R_p=4, 8, 12$ and 16). The results reveal that the use of quadruple counter-twisted tape with various combination showed that Nusselt number ratio (Nu/NU_o) decrease with Reynold number. The different pairs of quadruple twisted tape are full counter swirl (4T4), two across counter swirl (4T3), adjacent counter swirl (4T2) and fully co swirl pairs (4T1). The highest heat transfer rate was reported with 4T4 and lowest with 4T1. The friction loss ratio for 4T4 tape are 4%, 10% and 12% respectively higher compared with the 4T3, 4T2 and 4T1. The Nusselt ratio for quadruple V-finned counter-twisted tapes were increase with relative height. The quadruple V-finned counter twisted tape showed higher Nusselt number than quadruple twisted without V-fin. The friction factor ratio (f/f_o) increase with relative height and independent of Reynold number. It was found that the friction factor ratio was 63% higher with the V-finned counter-twisted tape compared to counter-twisted tape.

Hasanpour et al. (2016) investigated the heat transfer and friction factor in a concentric tube heat exchanger with modified twisted tapes in turbulent flow regime. The modified twisted include the pierced tape, V-cut and U-cut with twisted ratio 3, 5 and 7 were inserted in the inner corrugated tube. The hole diameter ratio for perforated tube was 0.11 ad 0.33, ratio of width to depth for U and V cut was 0.3to 0.6. The heat transfer increase with increase in Reynold number due to decrease in thermal boundary thickness by promoting the turbulence. The effectiveness of twisted tape decrease at lower Reynold number. The heat transfer decrease in corrugated tube by use of pierced twisted tape inserts. This decrease was due to drilled hole on twisted tape surface damage the swirl flow. It was found that the higher diameter ratio effect the swirl flow lead to straight flow compared to smaller diameter ratio.

Furthermore, heat transfer was found to be 1.30 and 1.80 times higher than the empty corrugated tube. The friction factor for V-cut and U-cut are higher for V-cut twisted tape than the corrugated tube. It was observed that friction factor decrease with increase in width ratio and decrease with diameter ratio.

Tamna et al. (2016) studied the heat transfer in a tube with double V-ribbed twisted tape insert. Experiment were performed for double V –ribbed twisted tape with varied parameter such as; relative height and relative pitch. It was founded that the Nusselt number for nanofluid with and without twisted tape was higher than the plain tube water as base fluid. The V-ribbed co-twisted tape shows 27-41% higher Nusselt number ratio and 1.4-1.47 times friction factor ratio that of twisted tape respectively. The friction factor for V-ribbed twisted tape was increase with the relative height. It was observed that the thermal performance tends to decrease with increase in Reynold number for V-ribbed co-twisted tape as well as for double twisted tape. The thermal performance was observed to increase 18.8-21.1% compared to twisted tape alone.

2.2 Liquid Additives

Addition of solvable additives and solid particles in single phase fluids increase heat transfer and reduces the surface tension.

Choi (1995) reported that the nanoparticle in base fluid were one method to increase the thermal conductivity of base fluid and reduce the pressure drop. It was found that nanoparticles have better stability than the microparticles.

Yang et al. (2005) investigated the convective heat transfer coefficient of a horizontal tube where graphite based nanofluid was used as working medium under laminar flow regime and constant heat flux condition. The experimental study was conducted on disc-shaped graphite nanoparticle obtained from different sources. The heat transfer coefficient increases with increase in Reynold number. It was observed that the heat transfer coefficient increase at lower temperature than the higher temperature. Furthermore, the graphite nanoparticles obtained from different sources having same concentration in base fluid have different heat transfer coefficient. It was found that the correlation developed by Li and Xuan for laminar flow regime of the nanoparticles predict heat transfer more than the experimental data.

Duangthongsuk and wongwises (2009) studied the convective heat transfer and flow characteristics of TiO₂-water in a horizontal double tube heat exchanger under turbulent flow regime. The experiment were conducted used TiO₂ nanoparticles of 21nm diameter at different temperature 15°C, 20°C and 25°C. The maximum enhancement observed was 6-11% higher for TiO₂-water nanofluid compared to base fluid. It was found that heat transfer coefficient was higher for lower temperature of nanofluid and higher mass flow rate of hot water. Moreover, the pressure drop was found to be decreasing with increasing in temperature of hot fluid and nanofluid. The friction factor for 0.2% vol. concentration shows no effect on pump power.

Zamzamian et al. (2011) investigated the heat transfer coefficient of Al₂O₃-ethylene glycol and CuO-ethylene glycol nanofluid flow in a horizontal double pipe heat exchanger for turbulent flow regime. The concentration of nanofluid of Al₂O₃-ethylene glycol was varied from 0.1%-1.0% weight and CuO-ethylene glycol was varied from 0.1%-0.5% weight were used in this study. It was found that the heat transfer increase 26% compared to the plain tube with Al₂O₃-ethylene glycol 1.0% wt. concentration. The maximum and minimum enhancement was observed 49% and 3%. This enhancement was due to the fact that the thermal conductivity of base fluid increase with nanoparticles and the chaotic movement of nanoparticles increase the energy exchange. It was observed that the temperature effect the enhancement of heat transfer coefficient of nanofluid compared to ethylene glycol. The heat transfer of CuO-ethylene glycol particle enhanced with the temperature of nanofluid due to the Brownian motion increase inside the nanofluid and viscosity of base fluid decreases.

Sajadi and Kazemi (2011) evaluated the convective heat transfer and pressure drop of TiO₂-water based nanofluid flow through a tube under the turbulent flow regime. The study were carried out with TiO₂-water nanofluid different concentration (0.05%, 0.15% and 0.25%). The experimental result showed that the ratio of heat transfer coefficient of nanofluid to the water decrease with increase in Reynold number. The heat transfer coefficient ratio was observed 1.19 and 1.22 times at concentration 0.05% and 0.25% of TiO₂ compared to water as base fluid. This showed that the nanofluid concentration have no significant effect on the heat transfer coefficient ratio. The pressure drop increase with the nanoparticle concentration in base fluid. The highest pressure drop was observed 25% more than the base fluid at lower Reynold number 5000 and highest concentration of nanoparticles 0.25% in base fluid. Furthermore, they developed a new correlation for single phase fluid.

Arulprakasajothi (2015) studied the heat transfer performance of TiO₂ /water based nanofluid in a horizontal tube. The different concentration (0.1%, 0.25%, 0.5% and 0.75%) of TiO₂ nanoparticle were studied. The experimental data were calibrated with the shah equation for laminar regime. The thermal conductivity enhancement of nanofluid depend on nano particle concentration, Brownian motion pH value, nanolayer, shape and size of nanoparticle suspended in base fluid. It was found that Nusselt number was increase 10%, 11.2%, 12% and 16.3% respectively at different concentration of TiO₂ /water (0.1%, 0.25%, 0.5% and 0.75%) compared to the water. The friction factor was observed to increase with concentration of nanofluid and decrease with Reynold number.

Anoop et al. (2009) investigated the effect of alumina nanoparticle on heat transfer characteristics flow through a tube under laminar flow region. The experiments were conducted on the alumina nanoparticle of average size 45 nm and 150nm. The heat transfer coefficient was higher for the nanofluid compared to base fluid and increase with concentration of nanoparticles in base fluid. The thermal conductivity for smaller particles was 6% at 45nm particle size and 4% for larger particles. The heat transfer coefficient for smaller nanoparticle size (45nm) was 25% and for larger particle size (150nm) was 11%. This showed that the effect of nanoparticle on heat transfer coefficient was beyond the increase in the thermal conductivity.

Hwang et al. (2009) studied the pressure drop and convective heat transfer coefficient of Al₂O₃ nanofluid flowing in a horizontal tube under constant heat flux. The concentration of Al₂O₃-water nanofluid varied from 0.01%-0.3% and Reynold number varied from 350-650 were studied. The value obtained for pressure drop of Al₂O₃-water at different concentration had good agreement with the Darcy equation for laminar regime. The maximum heat transfer coefficient was observed 8% at 0.3% concentration compared with the based fluid.

It was observed that the Shah equation in fully developed laminar flow regime failed to predict the heat transfer coefficient of Al₂O₃ –water nanofluid. The ratio of heat transfer coefficient of nanofluid to the heat transfer coefficient of water increase with the Reynold number in laminar flow fully developed region. The heat transfer coefficient of nanofluid was also effected by the nanoparticles dispersion, thermal conductivity under static and dynamic condition, particle migration and Brownian motion. The heat transfer coefficient was small effected by the thermal conductivity.

Khedkar et al. (2014) investigated the heat transfer coefficient of TiO₂-water based nanofluid for laminar flow regime in double tube heat exchanger under a constant heat flux. The concentration of TiO₂-water nanofluid was varied from 2.0%-3.0% in hot fluid flowing through the tube at flow rate of 1-3 lpm. It was observed that overall heat transfer coefficient of nanofluid at same Reynold number enhances with increase in concentration of nanoparticle in base fluid. The maximum enhancement was observed 47.36% at 3% concentration and Reynold number 3992 and with same Reynold number at 2% concentration the enhancement was 12% compared to water. The enhancement was due to loading and properties of nanoparticles. The enhancement increase 24%-33% with increase in temperature from 55°C-75°C. Furthermore, the enhancement increase with increase in mass flow rate from 1-3 lpm of hot side at same temperature about 4%-14%. These observation suggested that with increase in temperature, volume concentration and flow rate of hot fluid the increase in heat transfer coefficient of nanofluid

Godson et al. (2014) studied the heat transfer characteristic of silver-water nanofluid for turbulent flow in a shell and tube heat exchanger. The experiment were conducted at different heat flux 800 w/m² and 100w/m² and different concentration 0.01%, 0.03% and 0.04%. It was observed that heat transfer coefficient increase 12.4% at nanoparticle concentration 0.04% and Reynold number 25000 and at same concentration of nanofluid and Reynold number 5000 showed 6.08% compared to the water. The heat transfer coefficient increase with the mass flow rate and the particle concentration. The pressure drop was observed 12.84%, 11.15% and 16.22% higher compared to the base fluid at concentration 0.01%, 0.03% and 0.04% of nanoparticles. The pressure drop was increased with the Reynold number and the particle concentration of nanofluid.

Farajollahi et al. (2010) investigated the heat transfer of Y-Al₂O₃-water and TiO₂-water nanofluid in a shell and tube heat exchanger for laminar flow regime under the constant heat flux. The concentration of TiO₂-water nanofluid was varied from 0.15%-0.75% and Y-Al₂O₃-water 0.30%- 2% were studied in this experiment. The heat transfer coefficient for both the nanofluid increase at constant Peclet number compared to the water. The enhancement of heat transfer coefficient was 14%, 16%, 15% and 9% respectively compared to water using Y-Al₂O₃-water nanofluid. The heat transfer coefficient for TiO₂ nanoparticle enhancement was 11%, 24%, 16% and 13% respectively compared to the water. The heat transfer coefficient value decreases after optimum value of nanofluid concentration due to decrease in

thermal boundary layer thickness. The calculated Nusselt number for γ - Al_2O_3 -water and TiO_2 -water nanofluid by Xuan and Li correlation for turbulent flow showed higher value compared to experimental data.

2.3 Combination of Swirl Flow devices and Additives

Sadeghi et al. (2016) investigated the heat transfer and friction factor of Al_2O_3 and SiO_2 nanoparticles dispersed in a base fluid in a horizontal tube with helical twisted tape under a constant heat flux. The Al_2O_3 and SiO_2 nanoparticle of different shape and size (20-50nm) were used to study. The experiments with helical twisted tape of different twisted tape ratio 1.95, 2.93, 3.91, 4.89 and different volume concentration of nanofluid 0.5%-2.0% were undertaken under same condition. It was found that at same volume concentration and particle size for Al_2O_3 and SiO_2 nanoparticle. The Al_2O_3 -water nanofluid showed higher Nusselt number and lower friction factor as compared to the SiO_2 -water nanofluid. The maximum heat transfer coefficient was observed for higher concentration of nanoparticles. The heat transfer coefficient was influenced by the diameter of nanoparticles (20-50nm) at smaller size nanoparticles showed better result compared to bigger particles. The friction factor increase with decrease in twisted tape ratio and Reynold number.

Eiansa-ard et al. (2015) studied the heat transfer enhancement of TiO_2 nanoparticle suspended in water for turbulent flow in a heat exchanger with overlapped dual twisted tape. The concentration of TiO_2 -water nanofluid was varied from 0.07%-0.21% and overlapped twisted tape ratio was varied from 1.5-2.5. The Reynold number was varied from 5400-15200. The heat transfer was enhanced with decrease in overlapped twisted ratio. The enhancement was found to be 1.77-2.07 higher that for 1.5 twisted tape ratio as compared to water. Furthermore, the heat transfer coefficient for overlapped twisted tape was also higher from the single twisted tape insert. The Nusselt number increase with increase in TiO_2 concentration. The friction factor increased with increase overlapped twisted tape ratio. The friction factor were found 5.43, 4.95 and 4.55 times higher compared to the base fluid. Also found that with increase in volume concentration of nanofluid the friction factor increases.

Azmi et al. (2014) investigated that the heat transfer coefficient and friction factor of TiO_2 – water nanofluid flowing for turbulent flow regime in a tube under constant heat flux. The experiment were undertaken at different concentration 0.5%-3.0% of nanofluid and different

twisted tape ratio 5, 10 and 15. The heat transfer coefficient was increased with decrease in twisted ratio. Furthermore, the calculated Nusselt number using Manglik and Bergles for twisted tape insert coincided with the experimental Nusselt number. The heat transfer coefficient increase with increase in concentration of nanoparticles in base fluid up to 1.0% volume concentration. At higher concentration 1.5% shows decrease in heat transfer coefficient than 1.0% nanoparticles concentration. It was found that with increase in concentration of TiO₂-water more than 1.5% leads to decrease in heat transfer coefficient lower than the water. The Nusselt number value was higher for 1.0% concentration with twisted tape compared to 3.0%. The friction factor increased with decrease in twisted ratio and Reynold number.

Sun et al. (2016) studied the convective heat transfer coefficient and friction factor of Cu-water nanofluid in a tube with the built-in twisted belt inerts with a constant heat flux under the turbulent flow region. The experiments were used the different concentration of Cu nanoparticles and cetyl trimethyl ammonium chloride (CTAC). The nanofluid concentration increased from 0.1% to 0.5% result in increase in thermal conductivity and viscosity at the same condition. Also with increase in concentration of CTAC from 100-400mg/kg reduces the thermal conductivity and increase the viscosity which effect the heat transfer. The heat transfer coefficient was increase with volume concentration of Cu up to .4% with CTAC concentration 200mg/kg and .5% shows lower heat transfer than .4% under same condition. The volume concentration of Cu 0.4% and 200mg/kg CTAC showed lower value of friction factor compared to other Cu concentration. The heat transfer for nanofluid with the reverse ratio 2.5 shows better result from the reverse ratio 4.5.

Wongcharee and Eiamsa ard (2012) evaluated the heat transfer of CuO-water nanofluid in a horizontal corrugated tube with twisted tape under turbulent region. The experiment were undertaken the parallel and counter arrangement of twisted tape with relative to the corrugated tube. The different concentration 0.3%, 0.5%, 0.7% respectively of nanofluid were used with different twisted tape ratio. The Nusselt number were increase 4.7%, 7.7% and 11.8% respectively with particle concentration compared to base fluid. The nanofluid with twisted tape showed 51% to 168% improvement in heat transfer compared to the plain tube using water as fluid. It was found that the twisted tape arrangement in counter arrangement (CA) shows better heat transfer compare to the parallel arrangement (PA) of twisted tape.

The friction factor increase with the concentration of nanoparticle in base fluid. They observed that the friction factor increase 4.6% and 10% for CA compared to PA.

Nazari et al. (2015) studied heat transfer coefficient of Al₂O₃-water nanofluid flowing through the pipe fitted with metal foam. The different concentration 0.1%-1.5% of Al₂O₃-water and Reynold number 1000-6000 were undertaken in this study. The result of Nusselt number for plain tube were verified with the gnielinski equation and the friction factor were verified with Blasius equation have good correlation. The use of porous material inside the tube increase the heat transfer compared to the plain tube. The enhancement of heat transfer with porous material was observed more at higher Reynold number. Their results revealed that the Nusselt number increase 8-57% and the pressure drop increase 6-39% with increase the concentration of Al₂O₃-water nanofluid. The maximum Nusselt number increase 57% and pressure drop 37% at Re = 3704 compared to the plain tube. The Nusselt number ratio was found to increase with increase in particle concentration from .1-1.5% with the foam insert in the pipe compared to the plain tube.

Aliabadi et al. (2015) investigate that the heat transfer, overall performance and pressure drop of Cu-water nanofluid with varied twisted tape length insert flow in a horizontal tube. The experiments were conducted in turbulent range of Reynold number varied from 7500-15000 and nanoparticle concentration 0%, 0.1%, 0.3% by weight. It was founded that the twisted tape insert with non-uniform length namely low-high, low-high-low, high-low and high-low-high showed better results than the uniform twisted tape insert length. The maximum pressure drop was 149% using the low –high-low non-uniform length of twisted tape compared to plain tube. The friction factor of non-uniform twisted tape length increase 5.1%-22.2% compared to the uniform one. The overall heat transfer coefficient of non-uniform twisted length insert was 62.7% higher compared to plain tube and lowest value for high-low-high insert. The overall heat transfer ratio of low to high twisted tape insert length was 6.5%-49.3% higher than the uniform twisted tape value. The Nusselt number enhanced 19-106% with Reynold number and twisted –tape ratio compared to the plain tube. The overall enhancement ratio of low to high twisted tape insert with 0.3% nanofluid showed highest value compared to other twisted geometry and nanofluid concentration.

Prasad et al. (2015) investigated of twisted tape insert in a U-tube double pipe heat exchanger using Al₂O₃-water nanofluid. The experiment were conducted over Reynold number 3000-30000, nanoparticles range from 0.01% and 0.03% and twisted tape ratio 5-

20. The Nusselt number enhancement observed was 6.37% and 7.2% at 0.01% and 0.03% concentration at 30000 Reynolds number. The friction factor was increased 5.7% and 7.5% with Al_2O_3 0.03% concentration at Reynolds number 3000 and 30000. The Nusselt number increase 15.92% and 24.3% with nanofluid and twisted tape ratio 5 compared to the same nanofluid concentration. It was found that nanofluid with twisted tape increase Nusselt number 20.69% and 34.24% compared to the water in a tube. The friction factor was influenced by the twisted tape ratio, Reynolds number and the nanofluid concentration. The friction factor with twisted tape and nanofluid showed 1.29 times higher compared to without twisted tape.

Azmi et al. (2014) investigated the heat transfer of SiO_2 -water and TiO_2 -water nanofluid flowing through a tube under constant heat flux. The concentration of nanofluid 1.0%-3.0% and Reynolds number 5000-25000 were used in this study. The heat transfer coefficient was observed 15.3% and 4% at 1.0% concentration of TiO_2 -water and SiO_2 -water nanofluid with twisted tape ratio of 5. It was observed that at same twisted tape ratio and Reynolds number the heat transfer enhancement was 11.4% and 27.9% for 3.0% concentration of SiO_2 -water and TiO_2 -water nanofluid. The heat transfer coefficient was increased with decrease in twisted tape ratio from 93 to 5. Furthermore the calculated Nusselt number using Manglik and Bergles for different twisted tape ratio were coincide with the experimental Nusselt number. It was found that for lower concentration the TiO_2 nanoparticles showed better result than SiO_2 and the higher concentration the SiO_2 nanoparticle shows better result than the TiO_2 nanoparticles in higher concentration.

Xie et al. (2011) investigated on the heat transfer of shell and tube heat exchanger using artificial neural network approach (ANN). The results were compared with the experimental data and the correlation. The experimental were conducted on segmental baffles and helical baffles heat exchanger. The Reynolds number was varied from 3000-4000 in tube side and 300-7000 for shell side. The input layer was consist of eight neurons namely heat transfer rate, ΔT_{water} and ΔT_{oil} with reference to Reynolds number and inlet temperature in water and oil, diameter of centre tube, baffle pitch and total number of tubes and baffles. The ANN network was optimized to 8-6-5-3 configuration. It was observed that ANN predicts the result with deviation 2% with the experimental data and the correlation predicts value with 8% deviation. The ANN shows better result than the correlation.

Ermis et al. (2007) investigated on the heat transfer analysis of finned tube heat exchanger using multilayer feed forward network. The input layer consist of four neurons namely heat transfer, time, inlet HTF temperature and Reynold number. The output layer consist of one neuron namely total thermal energy storage. The 240 values from experimental data were divided into two sets first set consist of 200 value for train network and 40 case for verify the data. The network was optimized to 4-8-1 configuration. The total thermal energy storage was predicted with average MRE, regression (R^2) and standard deviation are 6.63%, 0.9919 and 7.78 respectively.

Hojjat et al. (2011) used neural network to predict the thermal conductivity of non-Newtonian nanofluid. In their study thermal conductivity of nanofluid were predicted using two different model one was for single type of nanofluid and other was for all three type of nanofluid. The first model was used to predict the thermal conductivity of each type of nanofluid with reference to the temperature and nanofluid volume concentration. The neural network structure was identical for all three γ - Al_2O_3 , TiO_2 and CuO nanofluid but the value of connected weight were varied. In second model thermal conductivity for all three γ - Al_2O_3 , TiO_2 and CuO nanofluid was predicted with reference to temperature, nanofluid volume percentage and nanoparticle thermal conductivity. The network was optimized to 3-2-1 for first model and 4-2-1 for second model. It was observed that ANN predicts the thermal conductivity of nanoparticles with average error was 1.6% and with maximum deviation was 5.8%.

Vaferi et al. (2014) applied the ANN model for predicting the nanofluid thermal behaviour for circular tube. In their study the nine variable such as critical temperature, critical pressure, molecular weight, acentric factor, nanoparticle size, volume fraction, temperature, heat flux, Reynold number were taken as neuron of input layer and the only output variable was heat transfer coefficient. The Reynold number was varied from 600-89000 and nanoparticles size was 20-100nm. The network was optimized to 9-10-1 configuration. It was found that the mean square error 1.7×10^{-5} , regression coefficient 0.99966 and absolute average relative deviation 2.41% for model experimental data for convective heat transfer coefficient. These value confirm the excellent agreement between the data predicted by ANN and the experimental value. The different ANN model such as Radial basis function (RBF), generalized regression (GR) and cascade-forward back propagation (CFB) were compared to multi-layer perceptron model on bases of AARD%, MSE and R^2 . The AARDs % was found

to be 2.41%, 2.46%, 3.01% and 14.59% respectively for MLP, CFB, RBF and GR for convective heat transfer coefficient. Their comparison clearly showed that two layer MLP network with ten hidden neuron shows best result.

Lecoeuche et al. (2005) developed an ANN model for online monitoring of a single tube heat exchanger at constant outer surface temperature. The numerical model and neural technique were studied the output of system from the input. The number of modulus which gave accurate solution of initial condition such as; input temperature and to compare the accuracy of numerical model the value are compared to steady state temperature. They observed that the initial and final temperature with unique time function was not sufficient to predict the temperature profiles for varied time. The neuron was optimized to three neuron in input layer, one neuron in hidden layer and four neuron in output layer. The ANN could be predict the output temperature at given input temperature. The predict ratio of ANN was estimated by compared the mean square error of actual output with the predicted value. At last it was showed that the deviation between the predicted output and experiment value was less than 0.1% and save time.

Vasickaninova et al. (2011) controlled the thermal process of heat exchanger using neural network predictive control structure and compared with PID controller. They developed neural network with three neuron were taken in the input layer namely diameter, density and specific heat and two neuron in output layer namely volume flow rate and heat transfer coefficient. The network with a 3-6-2 configuration control the tubular heat exchanger thermal process with integrated square error of 279.35 and the PID controller control with 304.7 integrated square error. The efficiency of the controller was verified with the simulation experiment. It was found that by chosen the efficient controller for the tubular heat exchanger significantly save the energy so the Neural network was practical application used for controlling the thermal process of heat exchanger. Their result showed that the ANN based controller is a good tool to control the temperature of outlet stream of heat exchanger to optimized value.

Tian et al. (2014) predicted the thermal performance of a parallel flow heat exchanger using multi-layer feed forward neural network. In their study the six neuron in the input layer namely dry bulb temperature, velocity of inlet air, wet bulb temperature, mass flow rate and pressure of refrigerant at inlet side was considered. The output layer consist of four neuron in hidden layer namely pressure drop and temperature for refrigerant and air leaving side. The

results reported that neural network with nine neuron in hidden layer predict the temperature and pressure drop in leaving side of air and refrigerant with root mean square error 0.002603, regression coefficient was 0.999928 and mean relative error value was in range 0.739168% for training data. ANN predicted value for parallel flow heat exchanger compare to the DPM data showed root mean square value 0.00463, regression value 0.9989 and relative error 1.06424%. These result showed that ANN model predict the thermal performance of heat exchanger with good level of accuracy.

Peng and ling et al. (2009) used multi-layer feed forward network for prediction of thermal characteristics of plate –fin heat exchanger. In this study the colburn and friction factor were predicted with reference to fin pitch, thickness, height, length and Reynold number of air side. The different neural network were tried such as 5-7-3-2, 5-6-4-2, 5-4-3-2, 5-6-2, 5-4-2 and 5-3-2 out of which 5-6-4-2 configuration was optimized. The neural network have relative error 4% and the mean square error less than 1.5% during the training period. The predicted value of colburn and friction factor was in range of 0-5%.The mean relative error for colburn and friction factor were 1.19% and 0.64% respectively. These above result showed that ANN model have high reliability and accuracy to predict the thermal characteristics of heat exchanger under varied operating condition.

Meybodi et al. (2015) predicted the viscosity of Al_2O_3 , SiO_2 , TiO_2 and CuO water nanofluid using the least square support vector machines. To develop model the 801 data set were used. The different type of learning method were in support vector machine such as linear, sigmoid, spline, polynomial and radial basis function. In their study the radial basis function was used to develop the least square support vector machines model. The viscosity of nanoparticle was influenced by nanoparticle concentration, temperature, size of particles and viscosity of base fluid. It was found that the subset value are divided into two category the training and testing value. The least square support vector model parameter was optimized by couple simulated anneal algorithm. The parameter value of LSSVM model were found by couple simulated algorithm was 0.5691 for σ_2 and 52.8976 for γ . Their result showed that the predicted viscosity value by LSSVM model have better agreement with the experimental viscosity value with 0.998 regression coefficient.

Peng and ling (2008) used the combination of genetic algorithm with back propagation neural network to optimize the plate and fin heat exchanger design. The logarithmic mean temperature difference was used to specify the heat exchanger dimension. In the heat

exchanger design the higher efficiency, smaller size and cost effective are important factor for designer. The combination of both help to minimized the weight of heat exchanger. It was found that use of genetic algorithm with back propagation reduce the weight about 54.8% compare to initial design. Also observed that the capital cost reduces with the reduction in size of heat exchanger. The total cost was effected by the pumping power required to pump the liquid through heat exchanger. The genetic algorithm method was compared with the combination of genetic algorithm with back propagation neural network. It was found that the iteration convergence was increase to 15 to 33 and the CPU time was increase 40.6% compared to combination of GA and BP method.

Esfe et al. (2015) predicted the thermal conductivity of hybrid nanofluid Cu/TiO₂-water/EG using artificial neural network. The Cu and TiO₂ nanoparticles were suspended in the base fluid by using two step method. The properties of hybrid nanofluid were study at different concentration varied from 0.1%-2% of nanoparticles at different condition 30°C-60°C. The two new neural network model were developed to predict the thermal conductivity of Cu/TiO₂-water/EG hybrid nanofluid with reference to the temperature and the concentration of nanoparticles in base fluid. The neural network was optimized to 2-5-5-1 configuration. It was found that the mean square error for this configuration was 2.62×10^{-5} and the regression coefficient was 0.999. The ANN predicted result were compared with the experimental value the mean square error was 2.62×10^{-5} and for line fitting second method have MSE value 1.33×10^{-6} and regression value 0.995. These result showed that the ANN neural network predict the thermal conductivity with high accuracy.

Zhang et al. (2010) developed a neural network for heat convection algorithm for heat exchanger and predict the Nusselt number for duct heat exchanger. The input layer consist of six neuron bulk air speed, height, and width, length of duct and inlet size and output layer consist of average Nusselt number. In their study to train the neural network the CFD result were used. The ANN model result were verified with the CFD simulation developed for other setups. It was observed that the ANN predicts the value accurately compared to CFD. Furthermore, they found that the ANN shows better result to predict the Nusselt number compared to available correlation for design heat exchanger, because ANN predicts the Nusselt number on the basis of flow rate and temperature condition and also it consider the surrounding factor into it model.

Tan et al. (2009) has predicted the thermal performance of fin –tube compact heat exchanger with air and water/ethylene glycol as a working fluid. The 359 data set were used to training the artificial neural network. The neural network had six neuron in input layer as ethylene glycol mass concentration, inlet obstruction, air and liquid mass flow rate and temperature of air. The output layer has only one neuron as overall heat transfer rate. It was found with 6-6-1 configuration of network predict the heat transfer rate with good accuracy. It was found that the neural network the predict data with 0.6%, 0.9% and 0.9% mean absolute error for training data, test and validation of data set. For the non-linear regression model the mean absolute error was 5.2%, 8.2% and 5.1% for test, train and validation data. Furthermore, they observed that non –linear regression model shows more error compared to ANN model. The result showed that neural network had higher accuracy to predict the heat transfer rate under the varied condition of temperature, flow rate and composition.

Chapter 3

Research Gaps and Objectives

3.1 Research Gaps

From the literature review, the following research gaps have been identified:

- The available standard correlation predicts the heat transfer and friction factor for heat exchanger with large deviation for nanofluids. To predict the heat transfer coefficient and friction factor with higher of accuracy the ANN model can be used. In ANN, detailed information of the process phenomenology is not required for model development.
- A limited literature review was available on Artificial Neural Network model to predict the heat transfer coefficient and friction factor for the double tube heat exchanger using TiO₂-water nanofluid with twisted tapes. The available literature are on modeling of heat exchanger using different nanofluid without twisted tape. So further research is required to investigate the effect of hybrid system
- The TiO₂-water nanofluid used in the heat exchanger for improving the heat transfer coefficient was proposed by many researchers paper but most of them used high concentration of TiO₂-water nanofluid and very little literature are available for use of lower concentration of TiO₂-water nanofluid. Therefore, further study is required to investigate the effect of TiO₂-water nanofluid at lower concentration.
- Many researcher have proposed that the different techniques for the improvement of the heat transfer coefficient but a very few literature are available on effect of these techniques on friction factor. This further requires to investigate the effect of heat transfer enhancement techniques on friction factor.

3.2 Research Objectives

Based on the critical literature review, the following objective have been set for the present work.

- I. To develop an ANN model for heat transfer coefficient and friction factor for double tube heat exchanger using the TiO₂-water nanofluid with different twisted tape ratio.
- II. To investigate the effect of volume flow rate of hot water, volume concentration of TiO₂-water nanofluid and twisted tape ratio on heat transfer coefficient and friction factor in concentric tube heat exchanger.
- III. To compare the thermal performance factor of nanofluid with swirl flow devices and without swirl flow devices.
- IV. To compare the friction factor of nanofluid with twisted tape and without twisted tape at same operating condition.

Chapter 4

Experimental Setup and Methodology

In the present work, the experimental study has undertaken to determine the thermal performance factor of TiO₂-water nanofluid, with and without twisted tape in a horizontal double tube heat exchanger. The experimental investigation of heat transfer coefficient and friction factor in a horizontal tube heat exchanger has undertaken for the following:

- I. Plain tube
- II. TiO₂ nanofluid
- III. Twisted tape of different twisted ratio
- IV. Combination of swirl enhancement device and TiO₂-water nanofluid.

4.1 Experimental Setup

The various components of experimental setup and swirl flow devices used to enhancement are as follows:

1. Support frame: All the component including the measuring devices such as manometer, rotameter and PID controller are mounted on it. Support frame material is made up of mild steel sheet and square conduit pipe.
2. Concentric tube heat exchanger: The heat exchanger consist of two concentric pipe. The inner pipe is made up of copper, because it has high thermal conductivity.

Inner pipe specifications are as,

Diameter of inner pipe	:	12 mm
Thickness of inner pipe	:	2.0 mm
Outer tube inner diameter	:	25.4 mm
Thickness of outer tube	:	3.0 mm
Length	:	1500 mm

The outer tube is made up of galvanized iron and it is insulated with the help of asbestos sheet and aluminium tape to reduce the convective and radial loss. Double tube heat exchanger consist of inner tube. Connectors are provide to the both ends of inner tube and twisted tape is inserted into the inner tube. The pictorial view of counter flow heat exchanger has been shown in Fig 4.1.



Figure 4.1: Pictorial view of counter flow heat exchanger

3. Hot fluid tank: A 50 litre capacity stainless steel tank was used to supply the hot fluid to double tube heat exchanger. A coiled element of 3KW has been used to heat the water and PID controller is used to maintain the water temperature 65°C . The hot fluid is flow through the inner tube of concentric tube and the cold water flow in annulus section of double tube heat exchanger. The hot water is recirculated in double tube heat exchanger. Asbestos sheet was used to insulate the hot water tank.

4. Heating element: A heating element of 3KW capacity was used to heating the fluid in hot tank. 220 V is require to operate a heater.

5. Cold water tank: The cold water tank supply the water at ambient temperature to the annulus section of double tube heat exchanger. The cold water after flowing through the annulus section of heat exchanger is drain out.

6. PID controller: The PID controller was used to maintain the hot fluid at constant temperature. The PID is connected to the heating element and help to maintain the temperature of water 65 degree Celsius. The PID controller have one sensor to check the temperature of hot fluid. Once the temperature of hot fluid reached to set value it cut off the power supply of the electric heater and maintained the required temperature and when the temperature fall below the set value the PID switch ON the heater. Thus the PID is used to maintain uniform heat flux. The pictorial view of PID as shown in Fig 4.2



Figure 4.2: Pictorial view of PID

7. Resistance temperature detector (RTD): The resistance temperature detector (RTD) PT100 was used to measure the temperature. The four RTD was used to detect the temperature of hot and cold fluid inlet and outlet. RTD measure the temperature range from -50 to 300°C .

The one end of RTD has been kept fixed in the connector of the double tube heat exchanger and other end is connected with the temperature display.

8. Temperature display/ selector switch: The temperature display is a device, which indicate the inlet and outlet temperature of hot and cold fluid with respect to RTD connected to it. The temperature display has 4 way switch to select the temperature reading required. The RTD were numbered according to displayer switch to reduce the measuring error. Calibrated RTD has been used to determine the reading of hot and cold fluid temperature of inlet and outlet side. The pictorial view of temperature displayer as shown in Fig 4.3.



Figure 4.3: Pictorial view of Temperature displayer

9. Pumps: The centrifugal pumps was used to circulate the hot and cold fluid through the test section and the annulus section of tube heat exchanger.

The centrifugal pump specifications are as,

Maximum head	:	1100 Lph
Maximum discharge	:	12m

The pumps are provided with control valve to bypass the fluid to maintain the flow rate in both section the inner tube side and the annulus section side. The pictorial view of pump is as shown in Fig 4.4.



Figure 4.4: Pictorial view of pump

10. Rotameter: The rotameter are used to measure the flow rate. The specification of rotameters used are as,

Rotameter for hot side : 1-5 LPM
Rotameter for cold side : 1-10 LPM

The control value is provided in each rotameter to control flow rate. The hot side flow rate has been varied from 1-5 LPM, while the cold side flow rate was kept fixed at 4LPM.

11. U-tube manometer: The U-tube manometer is use to measure the pressure drop across the inner tube of heat exchanger. A scale is mounted to indicate the height difference between both the sides across the inner tube of concentric tube heat exchanger.

4.2 Twisted Tape Inserts

Twisted tape insert are used to enhance the heat transfer coefficient by introducing swirl flow in the inner tube. A primary condition of twisted tape insert is that, the width of twisted tape should be smaller than inner tube diameter. The twisted tape having width 10 mm provide sufficient space between the tube wall and twisted tape. In present study the full length twisted tape has been used with thickness of 1mm. Tape was made from the galvanised iron, due to its easily availability and resistance to corrosion. The twisted tape was fabricated by holding one end in the chuck of lathe and other end is kept fixed in the tail stock. The constant pressure was kept on tail stock side to avoid the distortion of strip. Three twisted tape of different twisted ratio were fabricated and are shown in Fig 4.5.

Twisted Ratio 1 : 3.5
Twisted Ratio 2 : 4.6
Twisted Ratio 3 : 6.5



Figure 4.5: Pictorial view of twisted tape

4.3 Nanofluid's Preparation

The TiO₂-water nanofluid was prepared by using two-step method.

4.3.1 Estimation of the amount of Nanoparticles

The required amount of TiO₂ nanoparticles for preparation of TiO₂-water nanofluid was calculated by using the law of mixture formula. The weight of nanoparticle required for preparation of 1 litre TiO₂-water nanofluid of different concentration, using water as base fluid was calculated by following relation:

$$\% \text{ vol. conc.} = \frac{[\text{wt. of TiO}_2]}{[\text{wt. of TiO}_2/\text{density of TiO}_2] + [\text{wt. of water}/\text{density of water}]}$$

The amount of TiO₂ nanoparticle required to prepare nanofluid of different % volume concentration in 1 litre of water has been summarized in Table 4.1.

S.No.	Volume concentration (%)	Weight of TiO ₂ Nanoparticle (g)
1.	0.01%	0.3788
2.	0.025%	0.9470
3.	0.05%	1.894

Table 4.1 Volume concentration of TiO₂ with corresponding weight

4.3.2 Preparation of Nanofluid

The DEGUSSA P25 TiO₂ nanoparticle of average size 21nm and density 4.23 g/cm³ has been used for the present study. The pictorial view of TiO₂ nanoparticle has been shown in Fig 4.6.



Figure 4.6: Pictorial view of TiO₂ nanoparticles

4.3.3 Mixing of TiO₂-nanoparticles in water

Weighing balance was used to measure the required amount of nanoparticles. The measured amount of TiO₂ was dissolved in water using magnetic stir. The nanofluid prepared by this method is not stable and settled down due to gravity.

4.3.4 Adding surfactants to water

The suitable amount of surfactant has been added to base fluid to improve the stability of TiO₂-water nanofluid. The surfactant generally added is about one-tenth of the weight of TiO₂ at that concentration. Cetyl trimethyle ammonium bromide (CTAB) is used as a surfactant.

TiO₂-water nanofluid of different concentration 0.01%, 0.025% and 0.05% were prepared for measuring the heat transfer coefficient and friction factor in a double tube heat exchanger. The TiO₂-water nanofluid stirred for 30 minute and kept in a ultrasonic bath for 1 hour. The photographic view of TiO₂-water nanofluid magnetic stirred and ultrasonic bath has been shown in Fig 4.7.



Figure 4.7: Pictorial view of magnetic stirrer and ultrasonic bath.

The TiO₂-water nanofluid sample were prepared and observed that nano particle are not settle down. The pictorial view of TiO₂-water nanofluid has been shown in Fig 4.8.



Figure 4.8: Pictorial view of TiO₂ nanofluid.

4.3.5 Determination of properties of TiO₂ nanofluid

The thermophysical of TiO₂ nanofluid properties such as density, viscosity, specific heat and thermal conductivity effect the heat transfer coefficient.

Density of TiO₂-water nanofluid

The density of TiO₂ nanofluid is calculated by using Pak and Cho (1998) correlation equation.

$$\rho_{nf} = (1 - \Phi)\rho_w + \Phi\rho_{np}$$

Where Φ is volume fraction, ρ_p is density of particles and ρ_w is density of water.

Specific heat of TiO₂-water nanofluid

The specific heat is calculated by using Xuan and Roetzel correlation

$$c_{p, nf} = \Phi c_{p, np} + (1 - \Phi)c_{p, w}$$

Where $C_{p, nf}$ is specific heat of nanoparticle, C_{pw} is specific heat of water

Thermal conductivity

Thermal conductivity of TiO₂-water nanofluid sample was measured by using of KD2 pro. It consist of a sensor needle and microcontroller. The KD2 pro sensor was used to measure the thermal conductivity in range from 0.2-2 W/mK. During the thermal conductivity measurement assumption are made that the solution is homogeneous and initial temperature is constant. The pictorial view of KD2 pro is shown in Fig. 4.9.

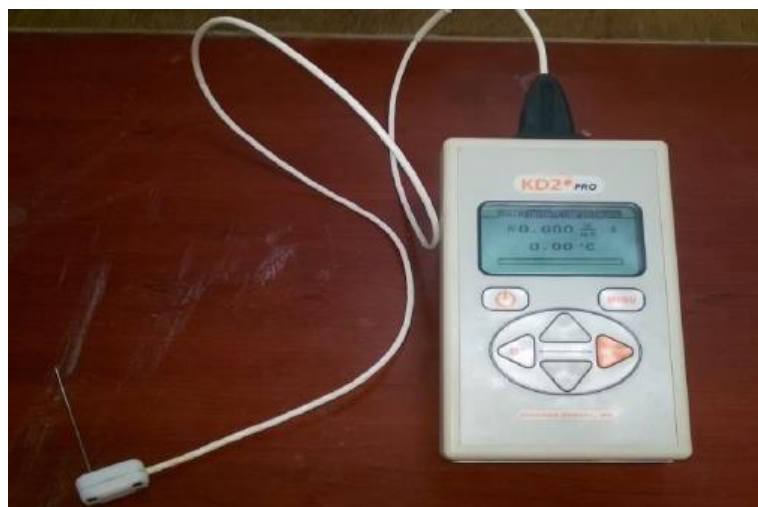


Figure 4.9: Pictorial view of KD2 Pro

Viscosity Measurements

The TiO₂-water nanofluid are prepared of volume concentration 0.01 %, 0.025 % and 0.05 % to measure the viscosity. The Brookfield viscometer is used to measure the viscosity of sample. The nanofluid at lower concentration assume to behave like Newtonian fluid. The TiO₂-water nanofluid was poured in the test sample cup and the spindle rotate in the nanofluid sample. The temperature of all the sample of TiO₂-water nanofluid is set to 65⁰c by the help of temperature controller. The Brookfield viscometer is used to measure viscosity, with accuracy of $\pm 0.1\%$. The Brookfield viscometer pictorial view is shown in Fig. 4.10.



Figure 4.10: Pictorial view of Brookfield viscometer

The schematic diagram and actual experiment setup are shown in Fig. 4.11 & Fig. 4.12.

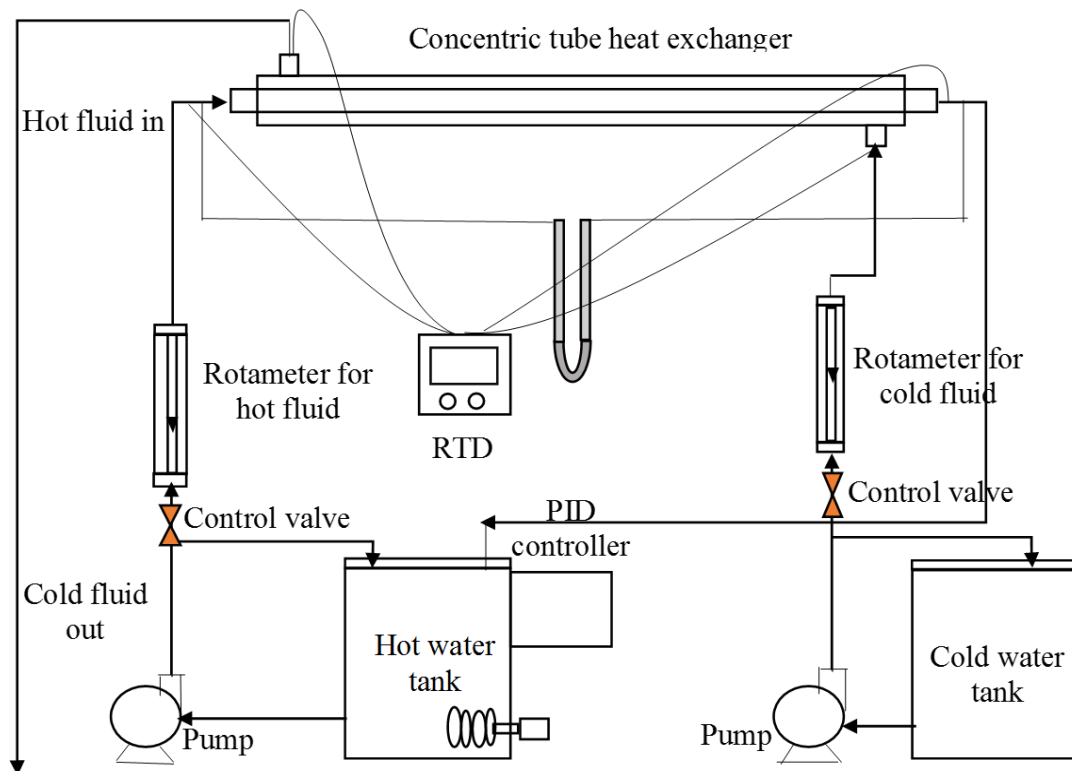


Figure 4.11: Schematic diagram of Experimental setup



Figure 4.12: Pictorial view of experimental setup

4.4 Experimental Procedure

1. Rotameter calibration: For calibrating both the rotameters a 1.5 litre beaker and stop watch is used. Volume of water calculated in one minute in the beaker is noted to calculate the volume flow rate. For each flow rate minimum of 3 reading are noted and then the average value is taken.
2. RTDs Calibration: All the RTDs are calibrated by inserted them in constant water bath and note the reading of each RTD. The one RTD value is taken as reference value and other RTDs are corrected accordingly.
3. Standardization of Experimental setup: The experimental setup is standardized by obtaining experimental value for Nusselt number and friction factor for plain tube and comparing the value of Nusselt number with the standard correlation.
4. Heat transfer coefficient: The heater is put ON to raise the temperature of water to 65°C and once the temperature reaches to 65°C it is maintained by the PID controller. The hot fluid tank is provided with a centrifugal pump to recirculate the hot water in inner tube of heat exchanger at volume flow rate of 1lpm. The cold water is recirculated in annulus section of heat exchanger in counter flow direction at ambient temperature and volume flow rate 4lpm.
5. Temperature reading: Temperature reading of hot and cold side fluid are recorded after 45 minutes when steady state condition achieved.

6. Friction factor calculation: The manometer is used to measure the pressure drop across the inner tube. The U-tube manometer uses mercury as a manometer fluid.

7. After completion of one cycle the mass flow rate of hot fluid was varied and all the procedure are repeated for different mass flow rate of hot water.

8. Twisted tape insert: The twisted tape ratio is calculated $=H/W$

H: pitch of twisted tape

W: width of twisted tape

The same procedure is used to calculate the heat transfer coefficient and friction factor and the experimental data is calibrated with the correlation for the twisted tape.

9. Similarly for different concentration the same approach is applied.

10. After calculating the heat transfer coefficient and friction factor for different twisted tape and different concentration the ANN is used to model and optimization of heat exchanger.

4.5 Artificial Neural Network Modeling

All ANN calculations have been carried out using Matlab 7.6 mathematical software with ANN toolbox. The following steps are involved for ANN modeling:

1. The parameter which effect the heat transfer coefficient and friction factor of heat exchanger are identify and take as input neuron in input layer.

2. The collected data were divided into training, validation and testing data.

3. The normalization of input and output data has been done.

5. The hyperbolic tangent 'TANSIG' has been used for mapping between input to hidden layer and the purely linear function has been used as mapping for hidden to output layer.

6. Optimization of number of neuron in hidden layer was done by minimizing mean square error.

8. Similarly, for friction factor the ANN model was developed using the twisted tape ratio, concentration of TiO₂-water nanofluid and the Reynold number as neuron in input layer and the friction factor as neuron in output layer.

9. The result from trained ANN model was extracted.

4.6 Variable Parameters in Experimental Study

To compare the effectiveness of various heat transfer enhancement method the experimental parameter varied are as follows.

1. Reynold Number: The Reynold number was varied using the control valves of the rotameter and the pump.
2. Twisted Tape Ratio: The different twisted tape ratio 3.5, 4.6 and 6.5 has been used in present study.
3. % Volume Concentration: Three different concentration 0.01%, 0.025% and 0.05% of TiO₂ water were used in present study.

4.7 Precautions

- 1 The twisted tape should kept at constant tension and rotated slowly during fabrication to prevent the distortion of twisted tape.
2. Rotameter should calibrated properly .So it gives exact reading of flow rate as small variation in the flow rate value effect the Reynold number and whole calculation.
3. RTDs should be calibrated and the correction may applied.
4. Pressure drop should be measured, when there is no air bubble in U-tube manometer.
5. The temperature reading should be only note when the steady state is achieved.

Chapter 5

Results and Discussion

In this section, an ANN model is developed to predict the heat transfer coefficient and friction for double tube heat exchanger using TiO₂-water nanofluid with twisted tape insert. The heat transfer coefficient has been enhanced using the TiO₂-water nanofluid and twisted tape to increase the thermal performance of a heat exchanger. This study includes the three different twisted tape ratio and different TiO₂-water nanofluid concentration. First we will discuss the ANN model for heat transfer coefficient for double tube heat exchanger. Then effect of different TiO₂-water concentration and different twisted tape insert on heat transfer coefficient and friction factor has been reported.

5.1 Heat Transfer Coefficient

5.1.1 Development of ANN model

The heat transfer coefficient of double tube heat exchanger is improved by using TiO₂ nanoparticle in base fluid and twisted tape to generate the swirl flow. In the present study an ANN model is developed to predict the heat transfer coefficient of double tube heat exchanger. The feed forward back propagation technique is used to train the neural network. The three- layer feed-forward neural network for heat transfer coefficient has been used as shown in Fig. 5.1. The input layer consists of five neuron namely as the Reynold number, twisted tape ratio, nanofluid concentration, input temperature of hot and cold side fluid. The heat transfer coefficient was taken as the output.

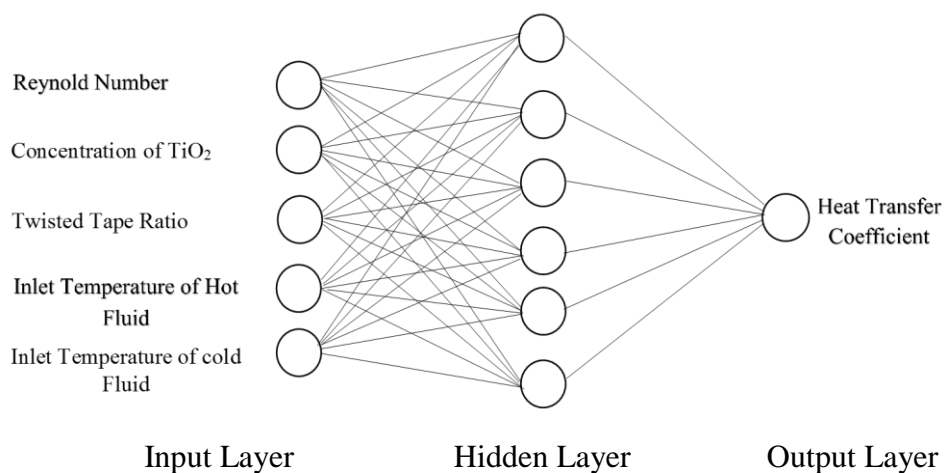


Figure 5.1: Feed Forward back propagation ANN model

The experiments were conducted on different twisted tape ratio and with different concentration of TiO₂-water and 96 data set were used for ANN modeling. The data set were divided into three group the training, validation and testing each contain 70%, 15% and 15% samples. One of the main steps in ANN modeling is to optimize the neuron in hidden layer. The mapping between the input layer and hidden layer was done by using sigmoid function and hidden layer to output layer by linear function. The regression plot for the network configuration 5-6-1 has been shown in Fig. 5.2(a).

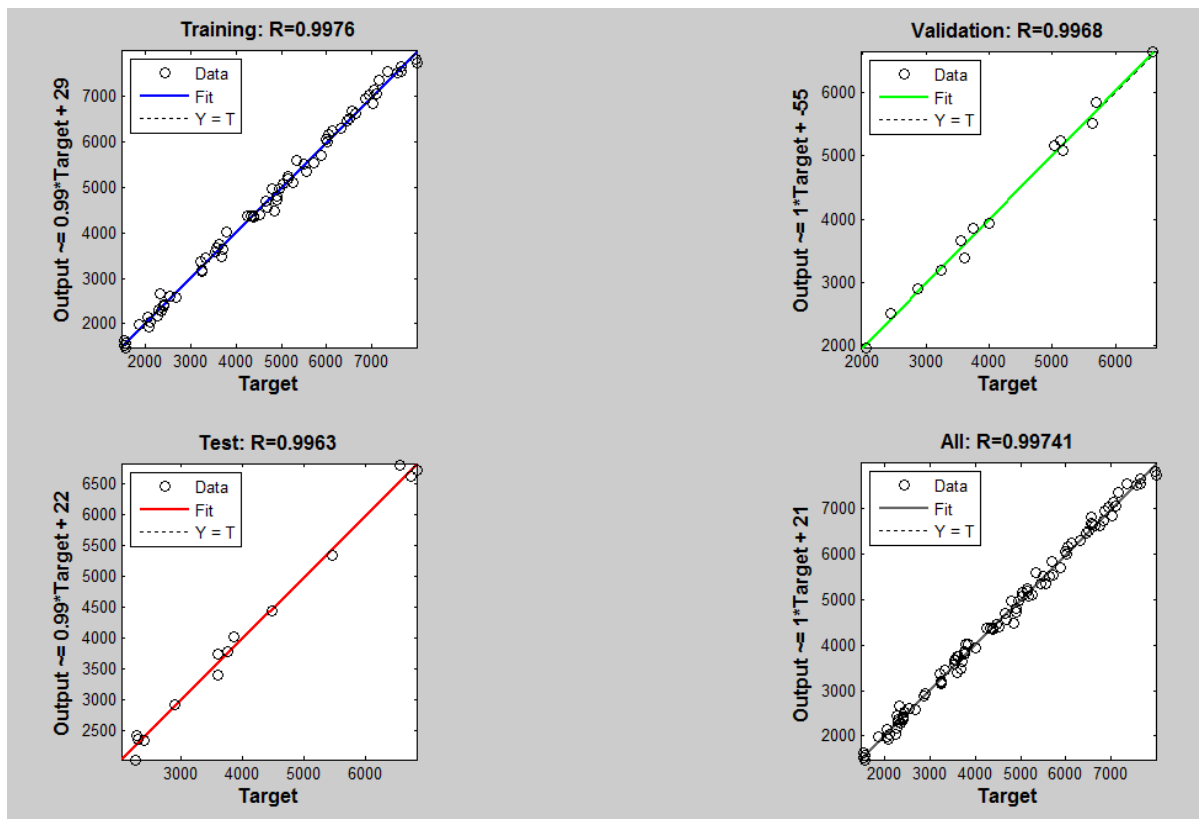


Figure 5.2: (a) Regression plot for ANN Model for heat transfer coefficient

The regression value for training, test and validation are 0.9964, 0.9963 and 0.9968. The minimum mean square error was shown by the 6 neuron in hidden layer and the configuration 5-6-1 was found to most accurate to predict the heat transfer coefficient. These regression and mean square minimum values shows the accuracy of ANN model and ready to simulate the output for corresponding input.

The prediction capability of ANN can be examined by Root Mean square error and regression value. The regression value shows accuracy of ANN model. The neuron in hidden layer was varied from 2-12 and the 6 neuron in the hidden layer was found to be optimum. The mean

square error (MSE) was used as error function. The Mean square error for different neuron in the hidden layer ranging from 2-12 are shown in Figure 5.2 (b). The mathematical expression for MRE and R^2 are as follow.

$$\text{MSE} = \frac{1}{N} \sum_{i=1}^N (h_i^{\text{exp.}} - h_i^{\text{cal.}})^2$$

$$R^2 = \frac{\sum_{i=1}^N (h_i^{\text{exp.}} - \Delta h)^2 - \sum_{i=1}^N (h_i^{\text{exp.}} - \Delta h)(h_i^{\text{cal.}} - \Delta h)}{\sum_{i=1}^N (h_i^{\text{exp.}} - \Delta h)^2}$$

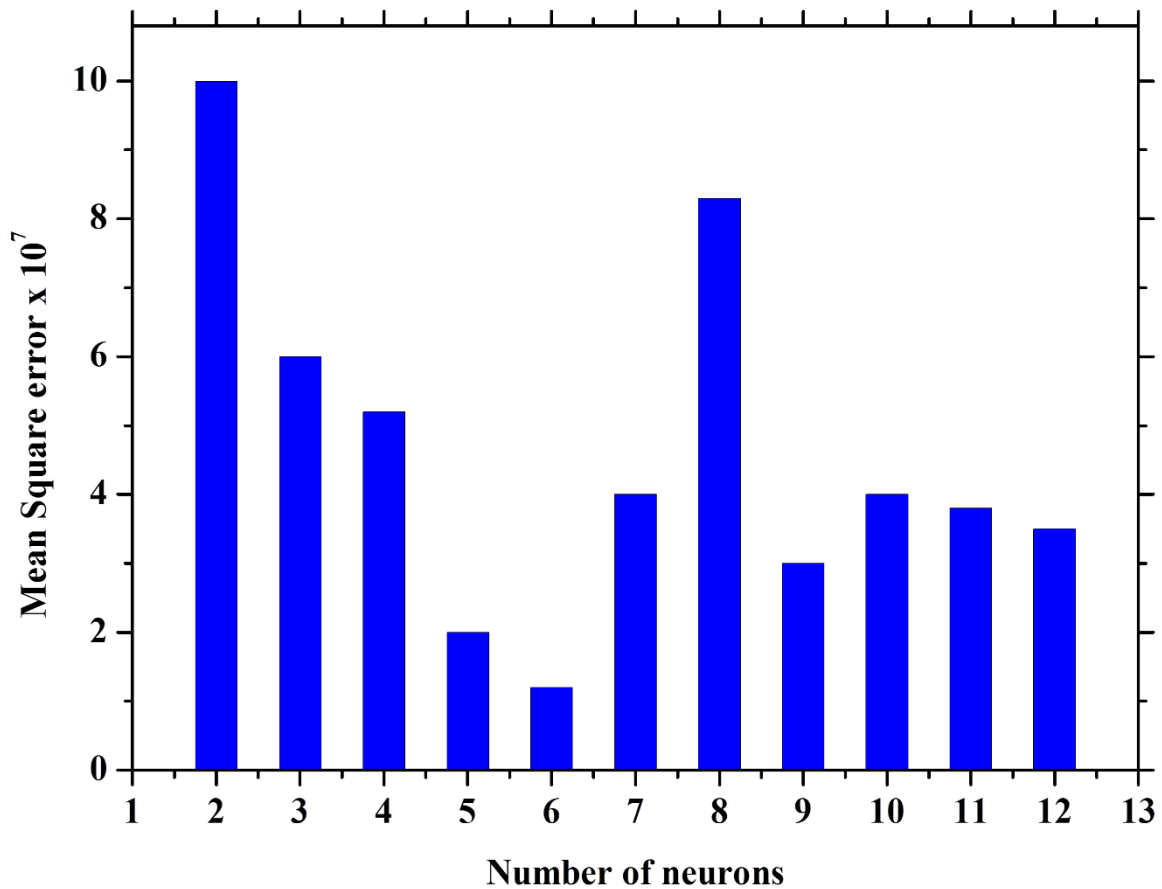


Figure 5.2: (b) Effect of hidden layer number of neuron of ANN model performance

5.1.2 Validation of Plain Tube

Before starting to determine the heat transfer coefficient of TiO_2 -water nanofluid the experimental setup of double tube heat exchanger is validated with the Dittus and bolter correlation. The deviation between the Nusselt number predicted by Dittus and bolter equation and the experimental data was $\pm 6\%$ which shows the reliability and accuracy of

the setup. Eiamsa-ard and promvong [2010], also reported the deviation between the Dittus Boelter and plain tube is ± 7.5 . Validation of Nusselt number for plain tube with the Dittus Boelter has been shown in Fig. 5.3. The sample calculation is shown in appendix A.1.

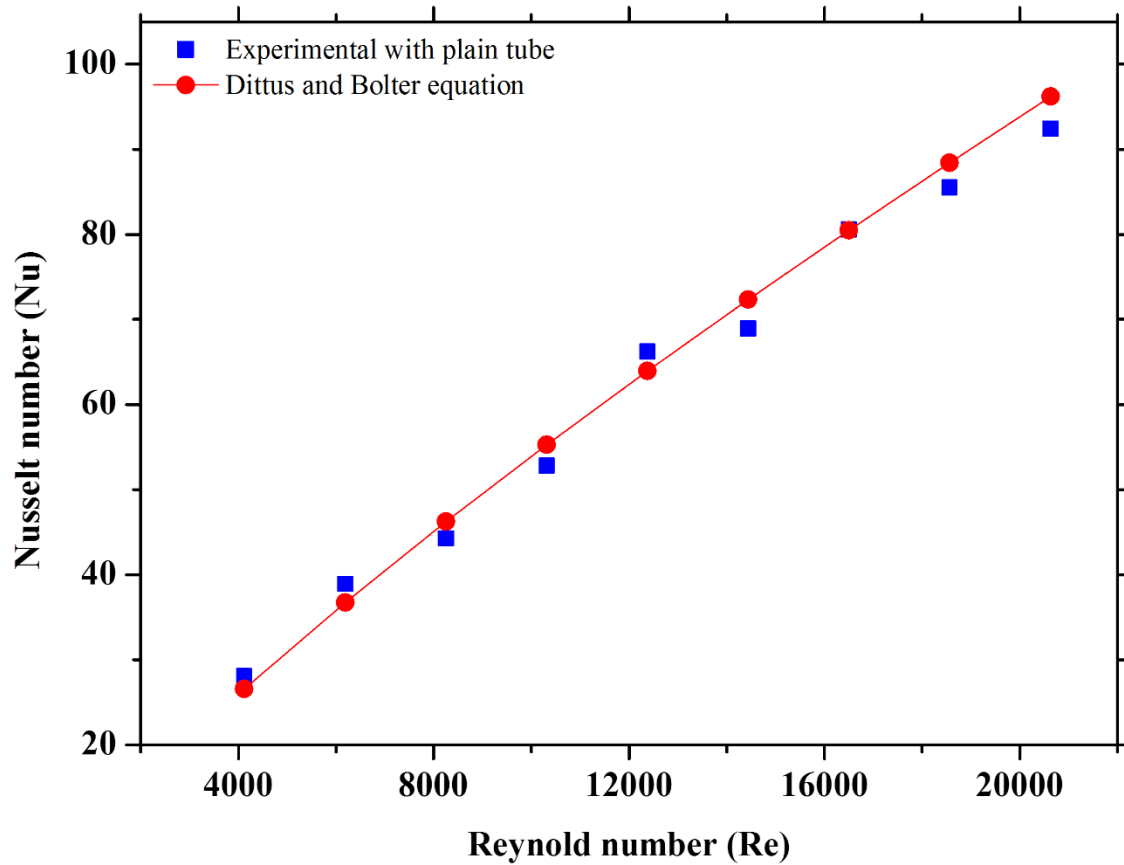


Figure 5.3: Validation of Nusselt number of Plain Tube with the Dittus Bolter.

It is observed that with increase in mass flow rate from 0.0163-0.0816 Kg/s of hot side fluid the exit temperature of hot side fluid increase which affects the heat transfer. The Nusselt number at mass flow rate 0.0163, 0.0816 kg/s was found to be 28.04 and 92.4. This shows that with increase in mass flow rate of hot side fluid the Nusselt number is enhanced.

The comparison of value predicted by optimal artificial neural network for heat transfer coefficient for plain tube with the experimental data has been shown in Fig. 5.4. The value of heat transfer coefficient predicted by the artificial neural network and the experimental data have small deviation as shown in Fig. 5.4. The regression value for optimal artificial neural network for training, test and validation data is 0.9976, 0.9968 and 0.99630. The proposed model predicts the heat transfer coefficient with 1×10^7 mean square error.

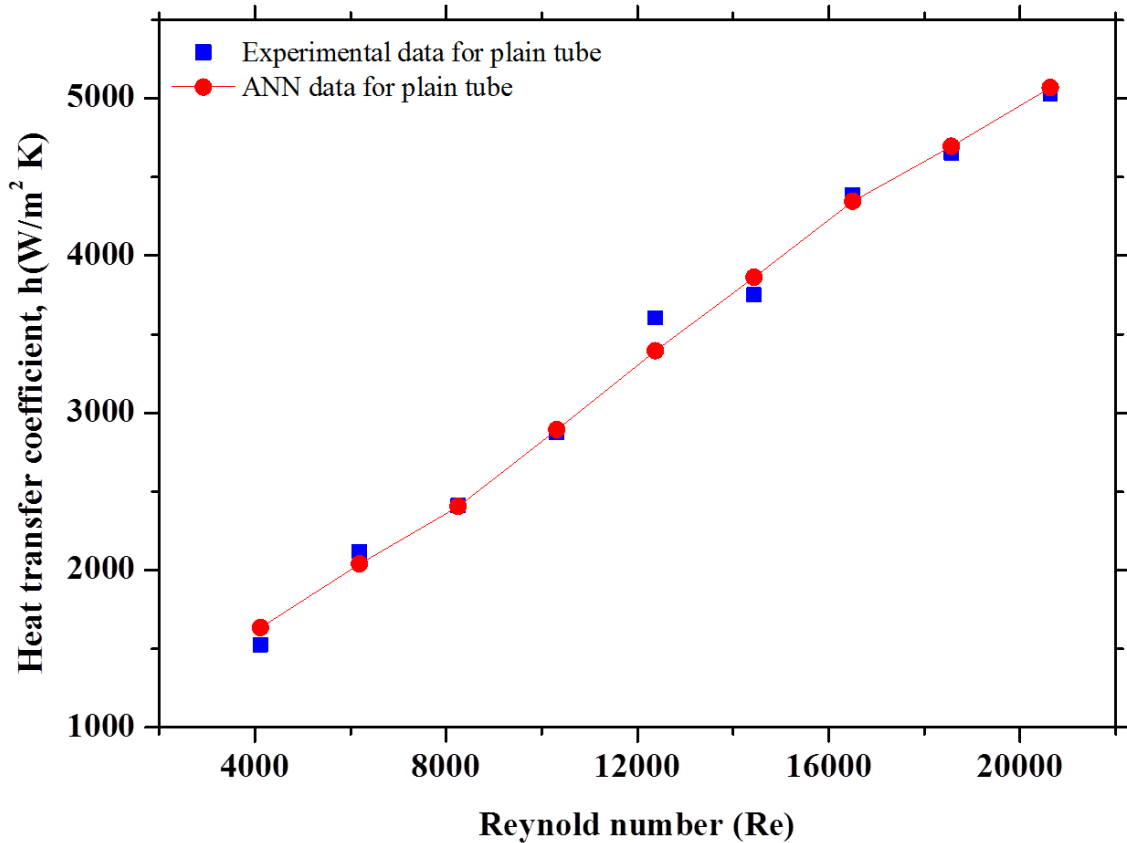


Figure 5.4: Comparison of ANN model with the experimental data.

5.1.3 Effect of Twisted Tape inserts on Nusselt number

The experiments are conducted with twisted tape ratio of 3.5, 4.6 and 6.5 at different mass flow rate of hot water vary from 0.016-0.081 Kg/s. The Nusselt number obtained from the experimental data is validated using the Manglik and Bergles equation for twisted tape for water as shown in Fig. 5.4. The result shows the maximum deviation between the experiment and equation is $\pm 11.5\%$. So the heat transfer coefficient of TiO_2 -water nanofluid with twisted tape can be determine accurately. The Nusselt number value increases with the twisted tape insert as compared to plain tube. The Nusselt number value increases with the decrease in twisted tape ratio. This is due to the fact that as twisted tape ratio reduces the swirl flow increase, better mixing of fluid and thinner boundary layer results in enhancement of heat transfer coefficient. It is observed that the Nusselt ratio (Nu_t/Nu_w) decrease with increase in mass flow rate. As increase in flow rate from 0.016-0.081 Kg/s the Nusselt number value also increase. Nusselt number ratio for the twisted tape 3.5, 4.6 and 6.5 is about 53%, 47.9% and 34.4% compared to plain tube.

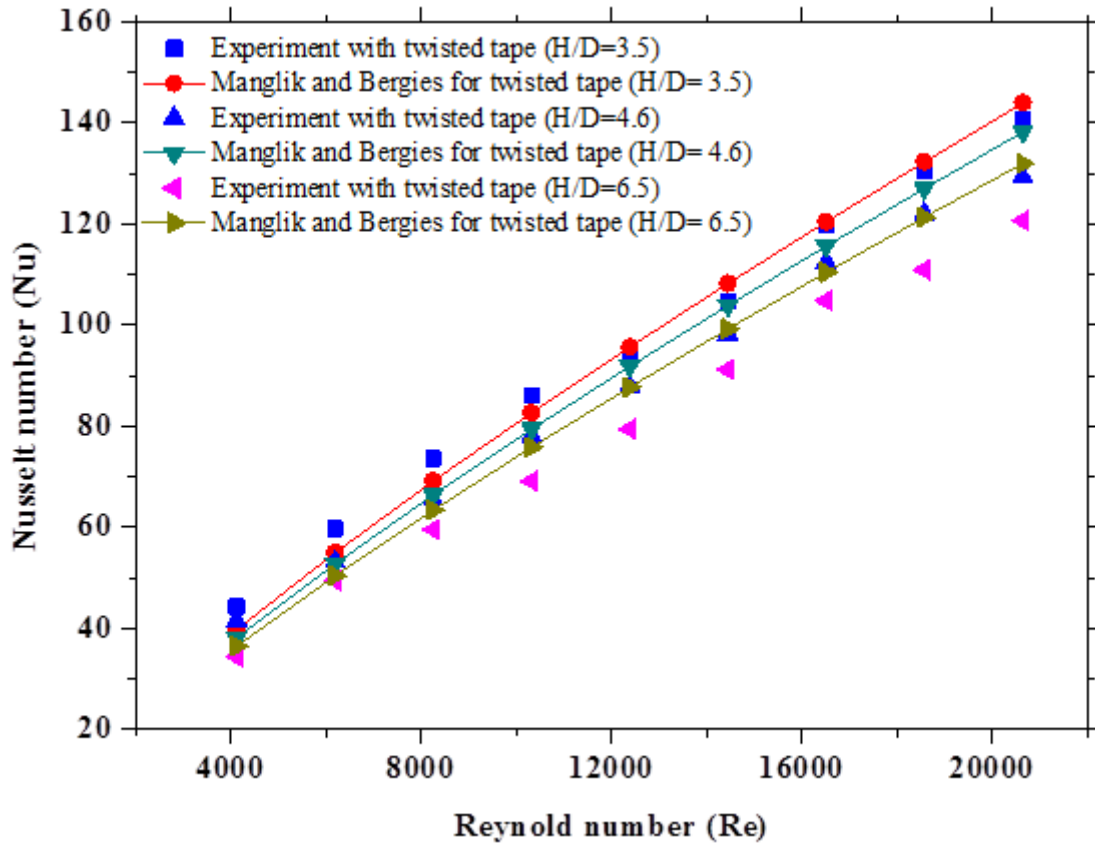


Figure 5.5: Validation of Nusselt number of Twisted Tape with Manglik and Bergies.

The ANN model was used to predict the heat transfer coefficient value for twisted tape insert with different twist ratio. The Nusselt number increase with decrease in twisted tape ratio and increase with Reynold number. The heat transfer comparison of experimental data of twisted tape and ANN model has been shown in Fig. 5.6. The deviation between the result obtained from the ANN and experimental data was found to be less than 5% for 5-6-1 configuration. The deviation between the correlation given by the Manglik and Bergles and experimental data is about $\pm 11.3\%$, whereas the deviation between the ANN predicted value and the experimental data is $\pm 10\%$, which shows that ANN model predicts the heat transfer coefficient accurately.

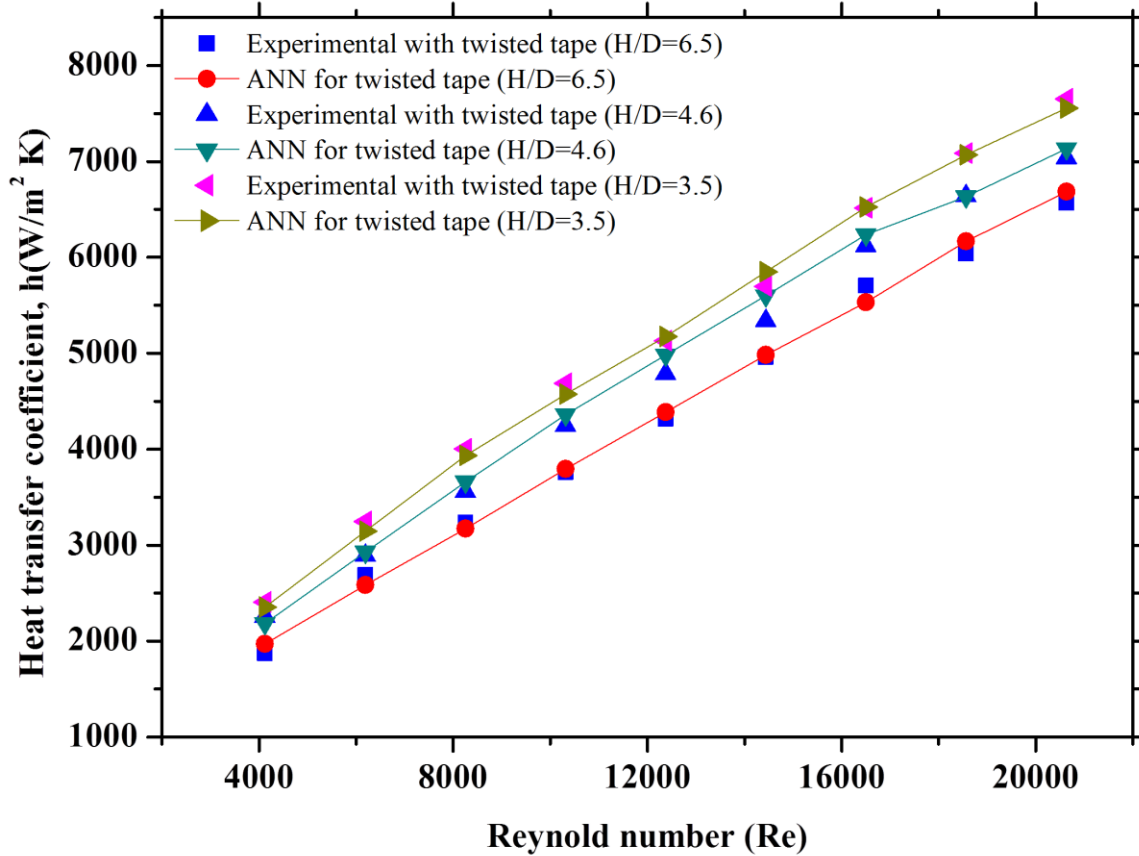


Figure 5.6: ANN model used to predict the heat transfer coefficient of twisted tape.

5.1.4. Plain Tube with TiO₂-water nanofluid.

The TiO₂-water nanofluid with different concentration 0.01%, 0.025% and 0.05% were used in plain tube for enhancement the heat transfer coefficient. Fig 5.7 shows the effect of different concentration of TiO₂-water nanofluid on heat transfer coefficient, experimentally as well as simulated by ANN model. It is observed that with the increase in TiO₂ concentration the value of Nusselt number increases. The heat transfer coefficient increases 2.4% and 3.2% for 0.025% and 0.05% TiO₂-water concentration compared to plain tube. Duangthongsuk and Wongwises [2009] also reported use of Degussa P25 TiO₂ nanofluid concentration 0.2% increased the heat transfer coefficient about 6-11%. From Fig.5.7 it is clear that with increase in concentration of TiO₂-water nanofluid the heat transfer coefficient enhanced, this shows the optimum range of TiO₂-water nanofluid concentration. The heat transfer coefficient increases with using the TiO₂-water nanofluid as base fluid due to fact that nanoparticles have higher thermal conductivity compared to water. Another reason is due

to chaotic movement of nanoparticles as reported by Choi [1995]. Due to chaotic movement of nanoparticles the heat transfer coefficient increases due to thinning of boundary layer.

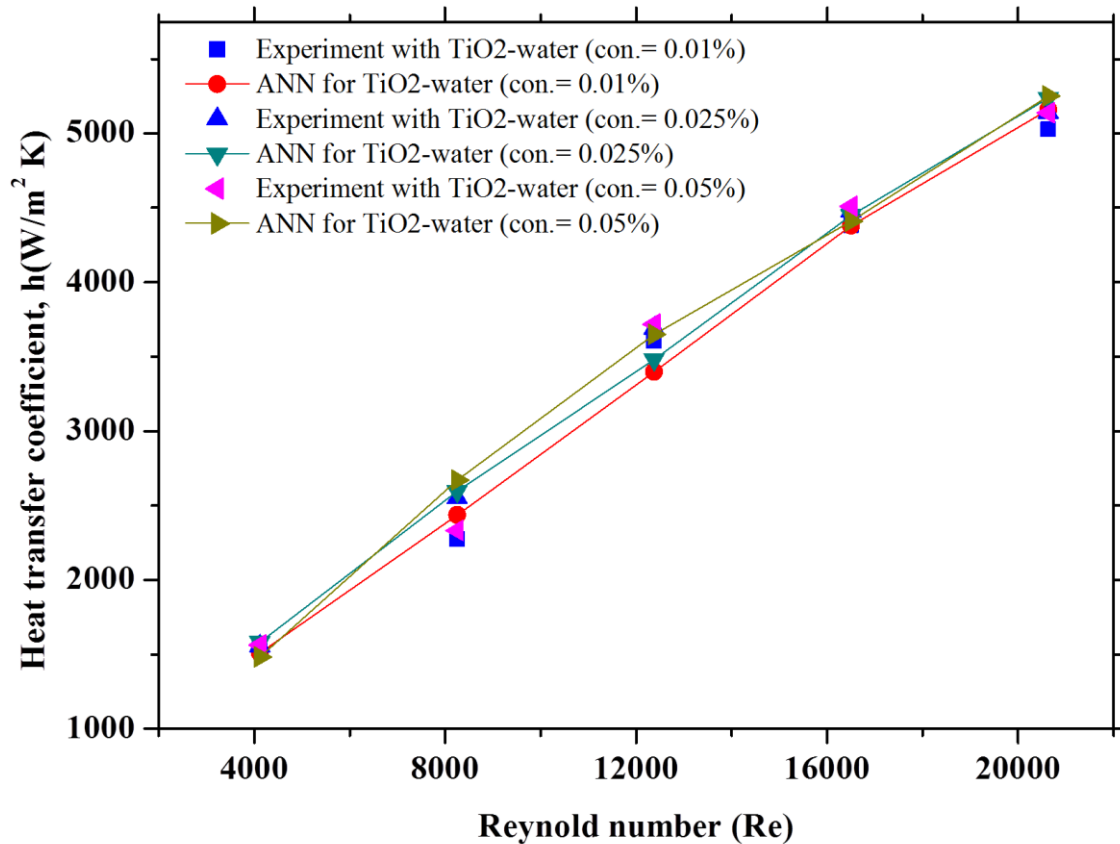


Figure 5.7: variation of heat transfer coefficient with TiO₂-water different concentration

The ANN results are compared with the experimental data for TiO₂-water different concentration in Fig. 5.7. From Fig 5.7 it is clear that, the deviation between the experimental and ANN prediction is very small.

5.1.5 Effect of TiO₂-water nanofluid with the Twisted Tape

The TiO₂-water nanofluid concentration 0.01%, 0.025% and 0.05% with twisted tape ratio 3.5, 4.6 and 6.5 insert were used to study the effect on heat transfer coefficient. The variation in heat transfer coefficient with different twisted tape ratio 3.5, 4.6 and 6.5 with 0.01% concentration of TiO₂ has been shown in Fig 5.8. It was found that using different twisted tape ratio 3.5, 4.6 and 6.5 with 0.01% TiO₂-water nanofluid, the heat transfer coefficient increases with decrease in twisted tape ratio. This is due to that as twisted tape ratio decreases the swirl increases and better mixing of fluid result in higher heat transfer coefficient.

Another reason is that twisted tape also increases the retention time of fluid in test section.

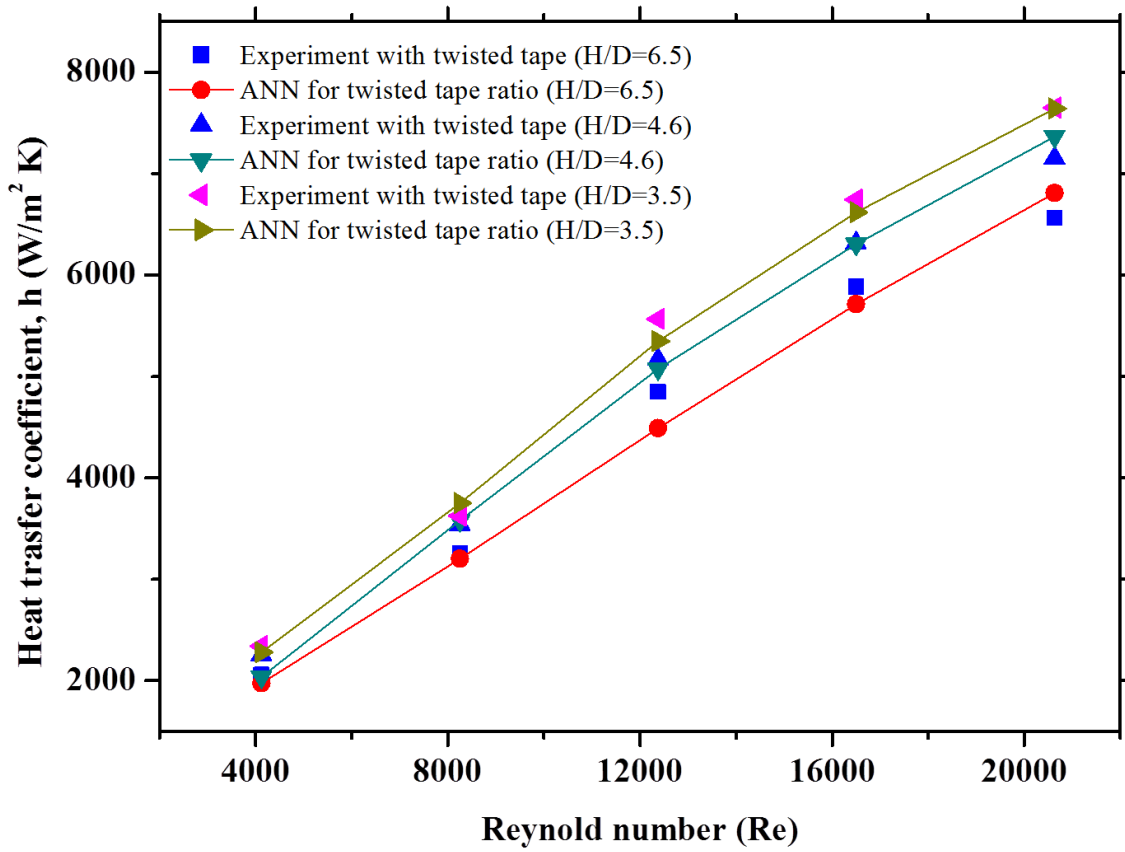


Figure 5.8: Variation of heat transfer coefficient with twisted tape ratio (H/D=3.5, 4.6 and 6.5) at 0.01% concentration of TiO₂-water.

It is observe that, the heat transfer coefficient at 0.01% TiO₂ concentration with different twisted tape ratio increases with decrease in twisted tape ratio from 6.5 to 3.5. The heat transfer coefficient increases 55.4%, 47.7% and 34.8% for twisted tape ratio (H/D=3.5, 4.6 and 6.5) respectively, at 0.01% TiO₂ concentration as compared to water. Azmi et al. [2014] reported that use of 1.0% TiO₂-water with twisted tape (H/D=5) enhances the heat transfer coefficient. The reason for heat transfer enhancement at same concentration with decreasing twisted tape ratio is that the swirl flow increase and the boundary layer thickness decreases. Another reason is that the chaotic movement of nanoparticles result in delay in development of boundary layer this result in higher heat transfer coefficient. The Fig.5.8 shows the comparison between experimental data and ANN predicted data of heat transfer coefficient for the 0.01 % TiO₂-water nanofluid with different twisted tape ratio. The deviation between the ANN model and experimental data is very small as shown in the Fig.5.8.

The comparison of experimental data and ANN model predicted data for the effect of heat transfer coefficient using 0.025% concentration of TiO₂-water with different twisted tape ratio (H/D=3.5, 4.6 and 6.5) has been shown in Fig. 5.9. It was found that heat transfer increases with decrease in the twisted tape ratio at same concentration this is due to the fact that decrease in twisted tape ratio result in increase in swirl flow, better mixing of fluid and thinning of boundary. The heat transfer coefficient increases 57% for twisted tape ratio 3.5 with 0.025% TiO₂ –water nanofluid as compared to plain tube with water. The heat transfer coefficient enhanced 49.9% and 35% for the twisted tape ratio 4.6 and 6.5 at same concentration as compared to water. The heat transfer decreases with increase in twisted tape ratio. Fig. 5.9 shows the variation of heat transfer coefficient with twisted tape ratio (H/D=3.5, 4.6 and 6.5) at 0.025% concentration of TiO₂-water. The Table A.1.4 shows the data for heat transfer coefficient experimentally as well as predicted by ANN model.

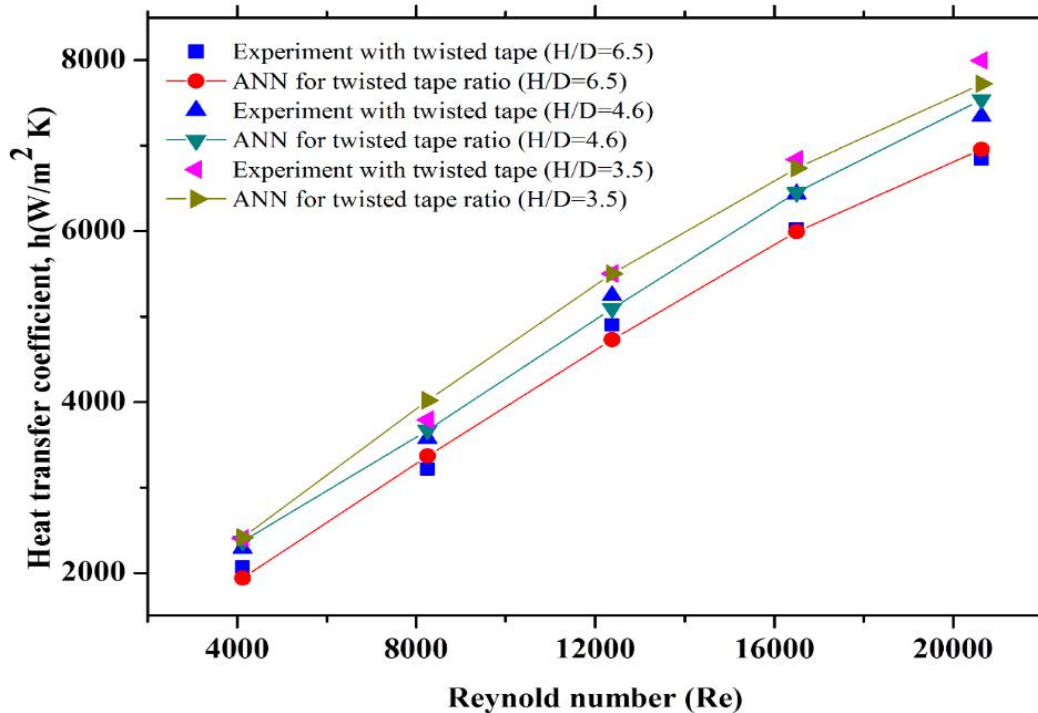


Figure 5.9: Variation of heat transfer coefficient with twisted tape ratio (H/D=3.5, 4.6 and 6.5) at 0.025% concentration of TiO₂-water.

The comparison of experimental data and ANN model predicted data for the effect on heat transfer coefficient using 0.05% concentration of TiO₂-water with different twisted tape ratio (H/D=3.5, 4.6 and 6.5) has been shown in Fig. 5.10. It was found that the heat transfer coefficient increases from 37.3% to 59% at same concentration with decrease in twisted tape ratio. The reason is that as twisted tape ratio decrease result in better swirl flow, better mixing of fluid and thinning of boundary.

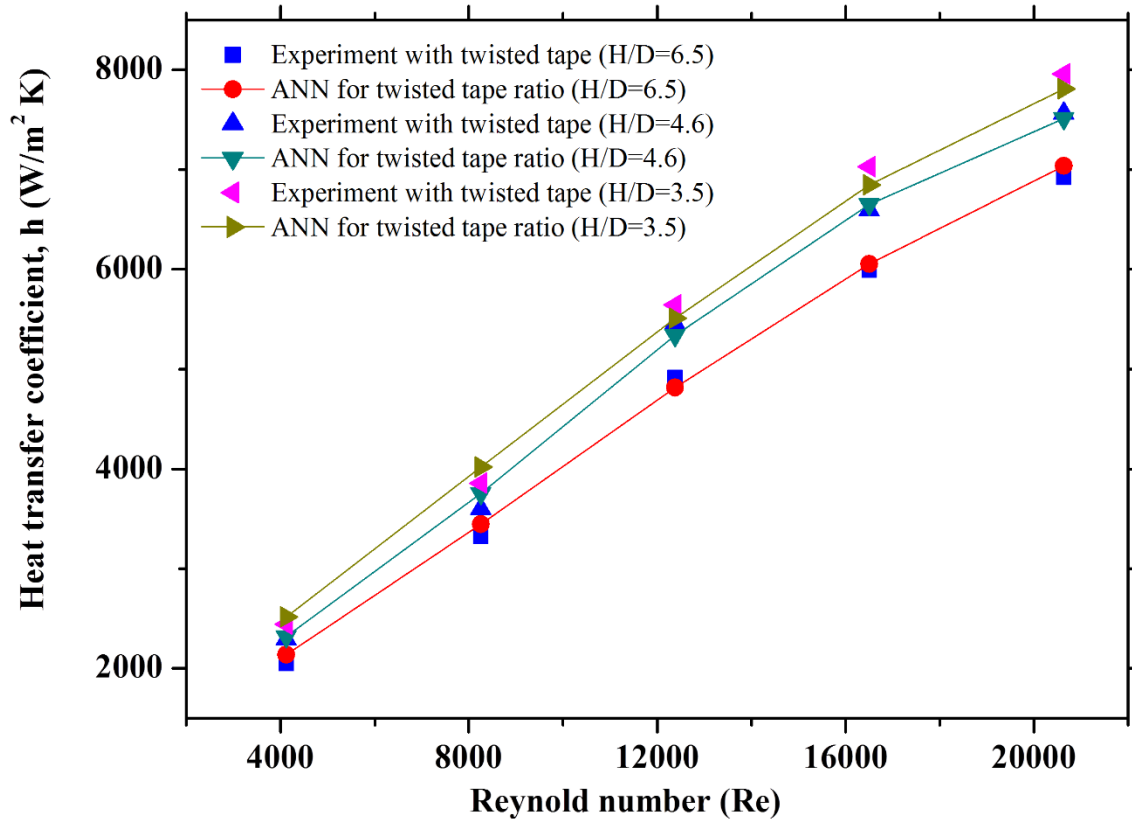


Figure 5.10: Variation of heat transfer coefficient with twisted tape ratio (H/D=3.5, 4.6 and 6.5) at 0.05% concentration of TiO₂-water.

5.1.6 Effect of Plain tube, TiO₂-water nanofluid, Twisted Tape with and without TiO₂-water nanofluid on heat transfer coefficient

The TiO₂-water nanofluid, twisted tape, with and without TiO₂-water nanofluid were used to study the effect on heat transfer coefficient by varying the Reynolds number. It is observed that the heat transfer coefficient increases with the increase in Reynolds number, concentration of TiO₂-water nanoparticles and decreases with the twisted tape ratio. The reason for enhancement is that at higher Reynolds number and higher loading of TiO₂-water nanofluid thinning of thermal boundary occurs. The comparison of TiO₂-water nanofluid, Twisted Tape with and without TiO₂-water nanofluid with the plain tube has been shown in Fig. 5.11

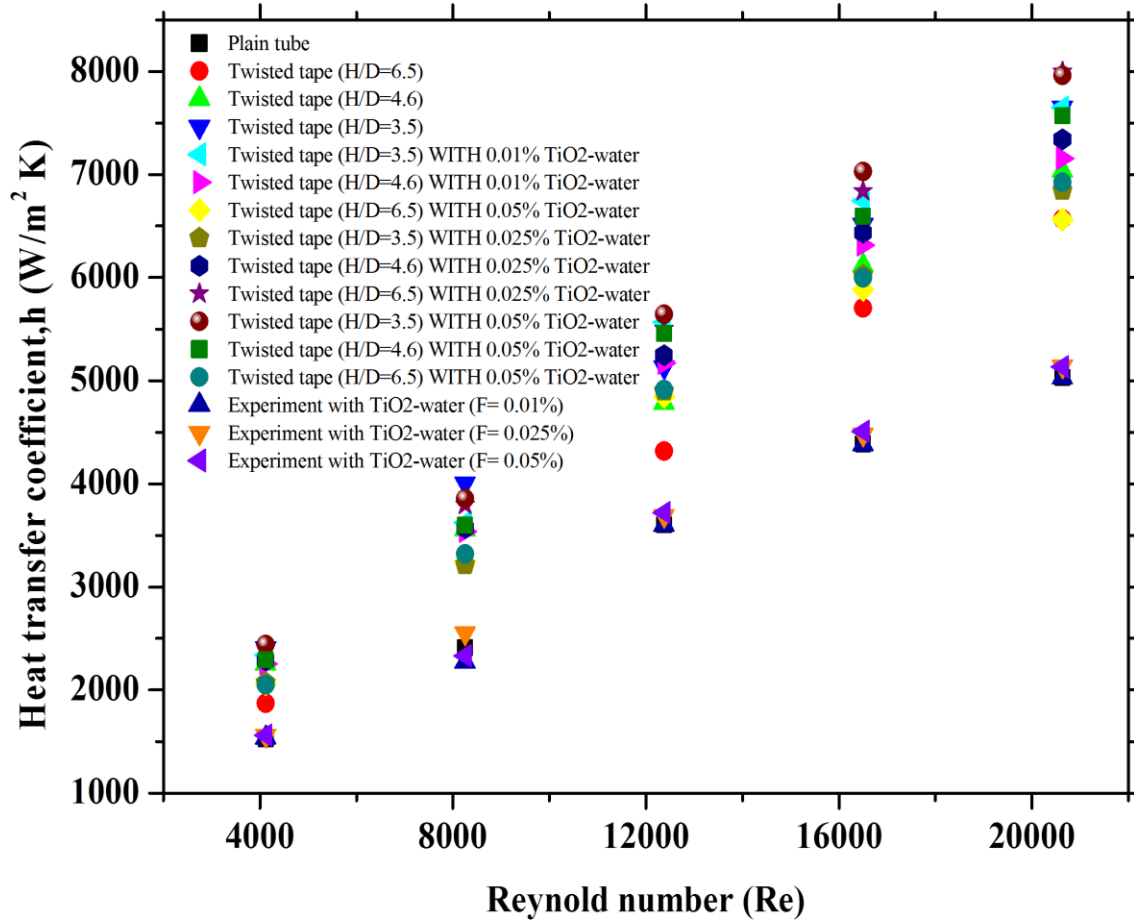


Figure 5.11: Comparison of different heat transfer coefficient techniques with the plain tube

5.2 Friction factor

5.2.1 Development of ANN model for friction factor

The heat transfer coefficient of double tube heat exchanger is improved by using TiO₂ nanoparticle in base fluid to improve its thermal characteristic properties and twisted tape to generate the swirl flow due to this friction factor increases. In the present study. An ANN model is used to predict the friction factor for double tube heat exchanger. The feed forward back propagation technique is used to train the neural network. The three- layer feed-forward neural network for heat transfer coefficient is performed as shown in Fig. 5.12. The input layer consist of four neuron namely as the Reynold number, twisted tape, nanofluid concentration and head difference. The friction factor were taken as neuron in the output layer.

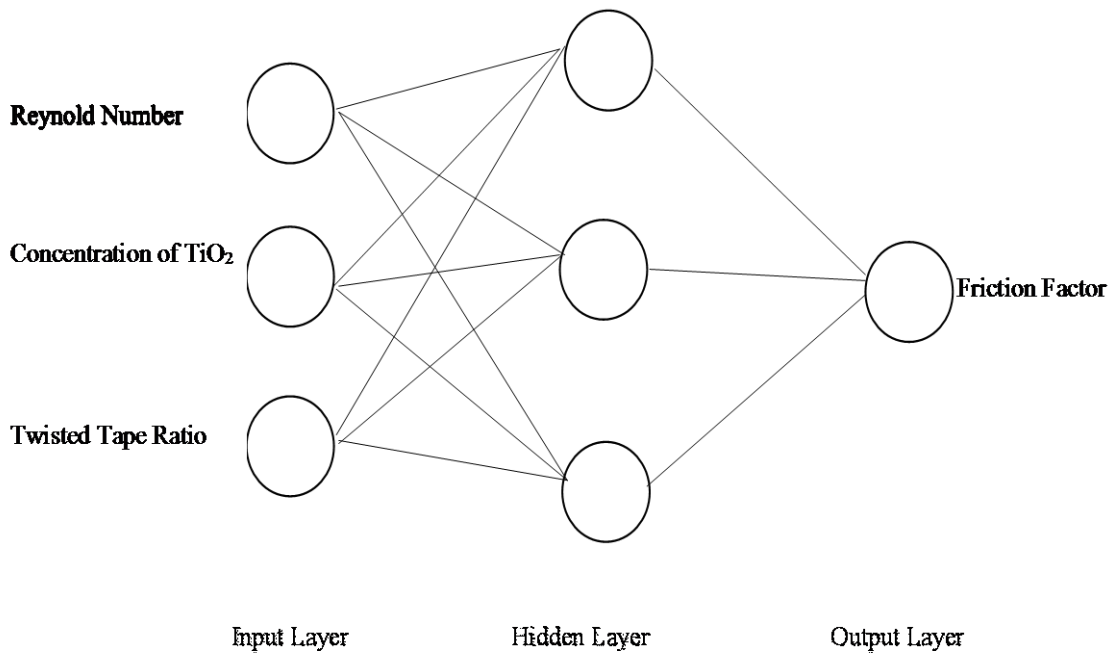


Figure 5.12: Feed forward back propagation neural network

The experiments were conducted and 96 data set were used for developing the ANN model. The data set were divided into three group the training, validation and testing, each contains 70%, 15% and 15% samples. The mapping between the input layer and hidden layer has been done by using sigmoid function and hidden layer to output layer by linear function. The regression plot for the network 3-3-1 has been shown in Fig. 5.13.

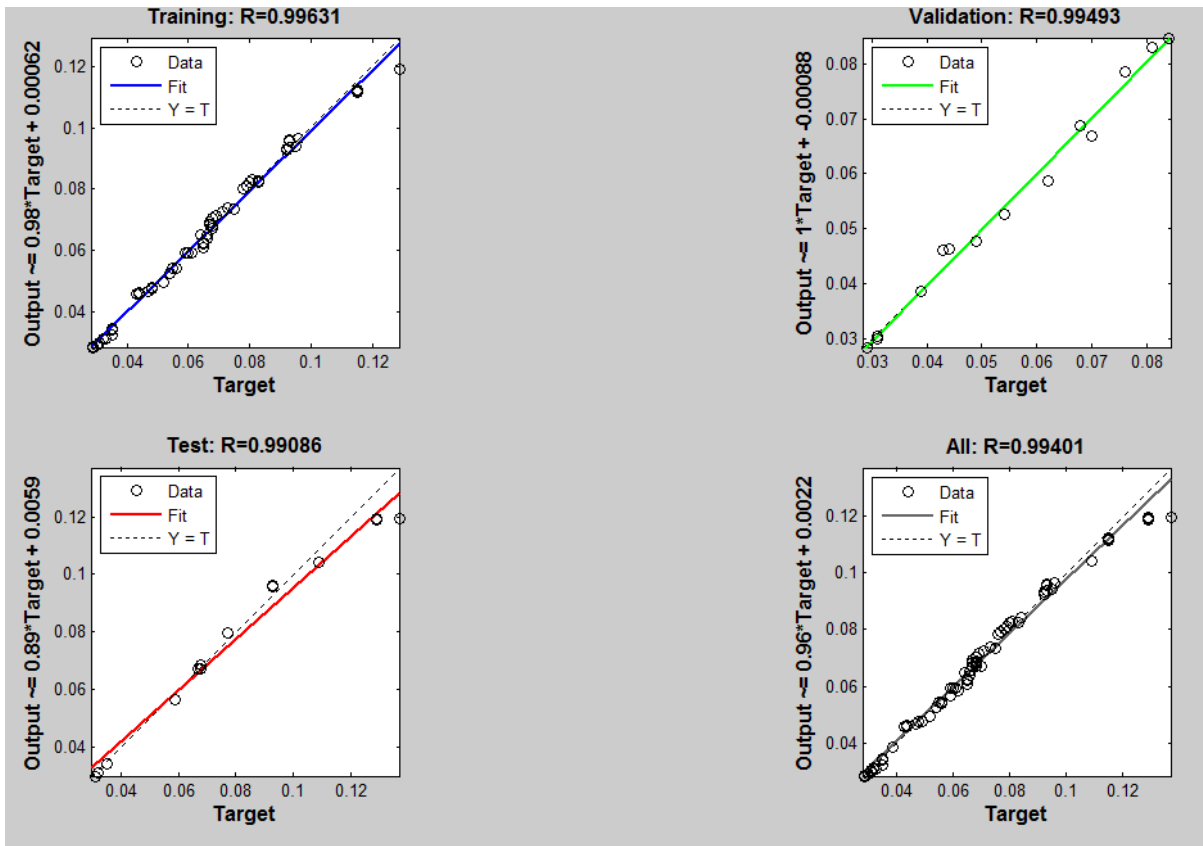


Figure 5.13: (a) Regression plot for ANN model for friction factor

The regression value for the training data, test and validation data is 0.998, 0.9972 and 0.9979. These regression values show the accuracy of ANN and ANN can be used to simulate the friction factor for double tube heat exchanger.

The prediction capability of ANN can be examined by Root Mean square error and Regression value. The mean square error for 3-3-1 configuration is 2.2×10^{-3} . The number of neurons in the hidden layer were varied from 2-10 and the 3 neurons in the hidden layer were found to be optimum. The Mean square error for different neurons in the hidden layer ranging from 2-10 is shown in Figure 5.13 (b).

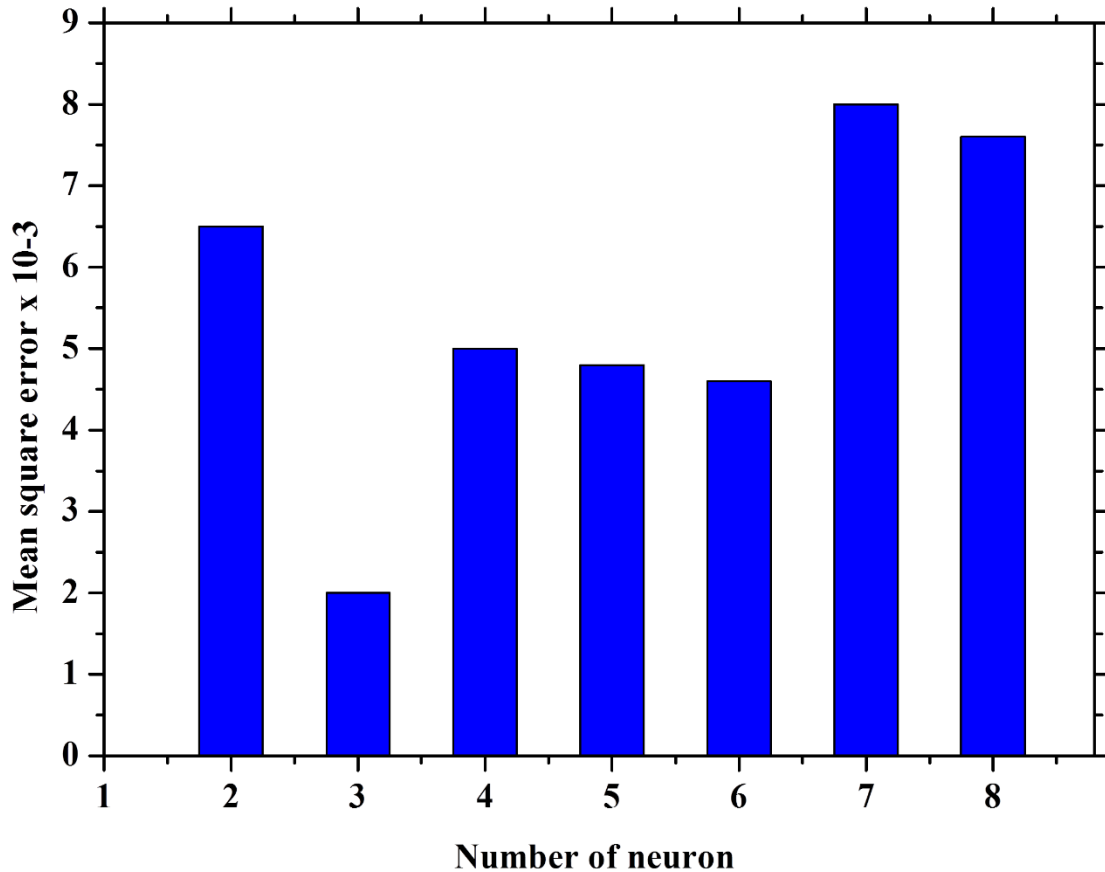


Figure 5.13: (b) Effect of hidden layer number of neuron of ANN model performance

5.2.2 Validation of Plain Tube

Before starting to determine the friction factor of TiO₂-water nanofluid, the experimental setup of double tube heat exchanger was validated with the Blasius equation with maximum deviation of $\pm 10\%$. This deviation shows the reliability and accuracy of the setup. Eiamsa-ard and promvongue [2010], also reported that the deviation in the experimental friction factor was $\pm 12\%$ from the friction factor predicted by Blasius equation. So the friction factor of the TiO₂-water nanofluid is determine accurately. Validation of friction factor for plain tube with Blasius equation has been shown in Fig. 5.14. As mass flow rate increases from 0.016-0.081 Kg/s the friction factor decrease from 0.043-0.029.

The friction factor was predicted by ANN model with 3-3-1 configuration. The comparison of experimental friction factor and the artificial neural network has been shown in Fig 5.15. The ANN predicts the friction factor with higher accuracy as the ANN predicted data and the experimental data overlap each other as shown in Fig 5.15.

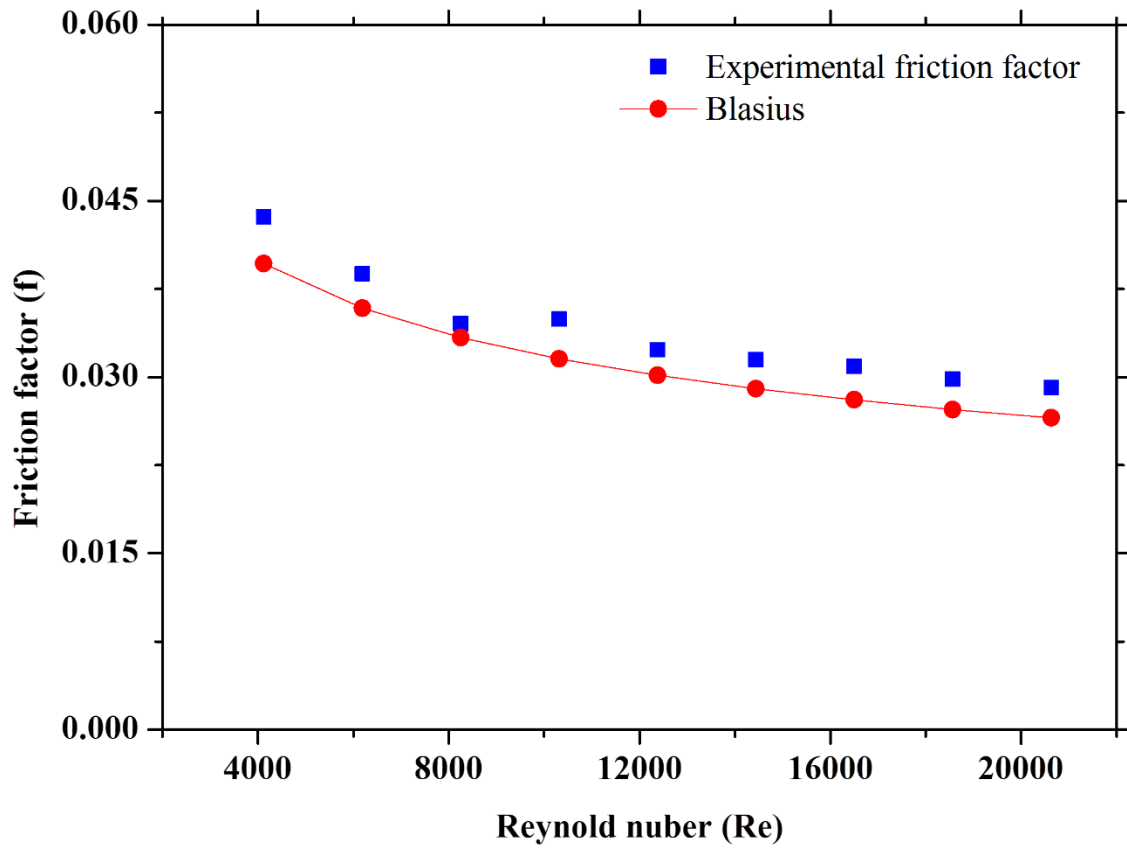


Figure 5.14: Validation of friction factor of Plain Tube with the Blasius equation. The ANN model configuration 3-3-1 predicts the friction factor with high accuracy as shown in Fig.5.15.

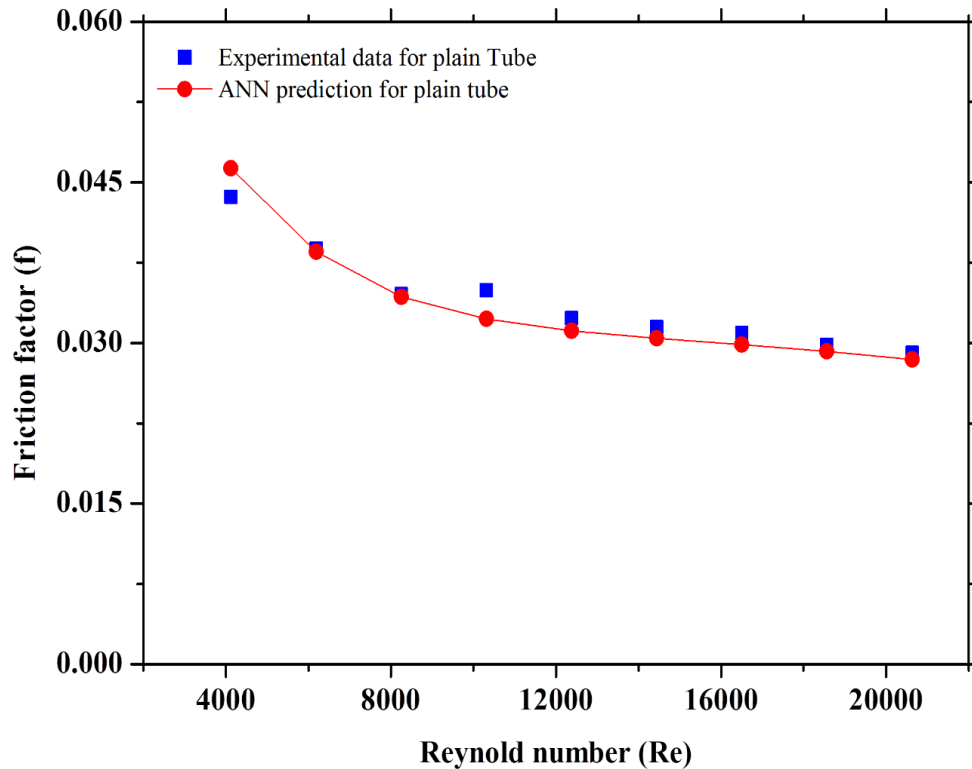


Figure 5.15: Comparison of friction factor of Plain Tube with the ANN model.

5.2.3 Effect of Twisted Tape inserts on friction factor

The experiments were conducted with twisted tape ratio of 3.5, 4.6 and 6.5 at different mass flow rate of hot water, from 0.016-0.081 Kg/s. The friction factor enhances 1.95, 1.63 and 1.14 times compared to water in plain tube. It was observed that with increase in Reynold number the friction factor decreases. It was observed that with decrease in twisted tape ratio the friction factor decrease due to the fact that as twisted tape ratio decrease the surface area increases, which perturbed the flow in the tube. Comparison of experimental friction factor with predicted by Smithberg has been shown in Fig. 5.16 (a) and have good agreement. Azmi et al. [2010] also reported that the experimental friction factor and Smithberg prediction has good agreement. Fig 5.16(b) shows the effect of different twisted tape on the friction factor and compare the result of twisted tape obtain experimentally and ANN model.

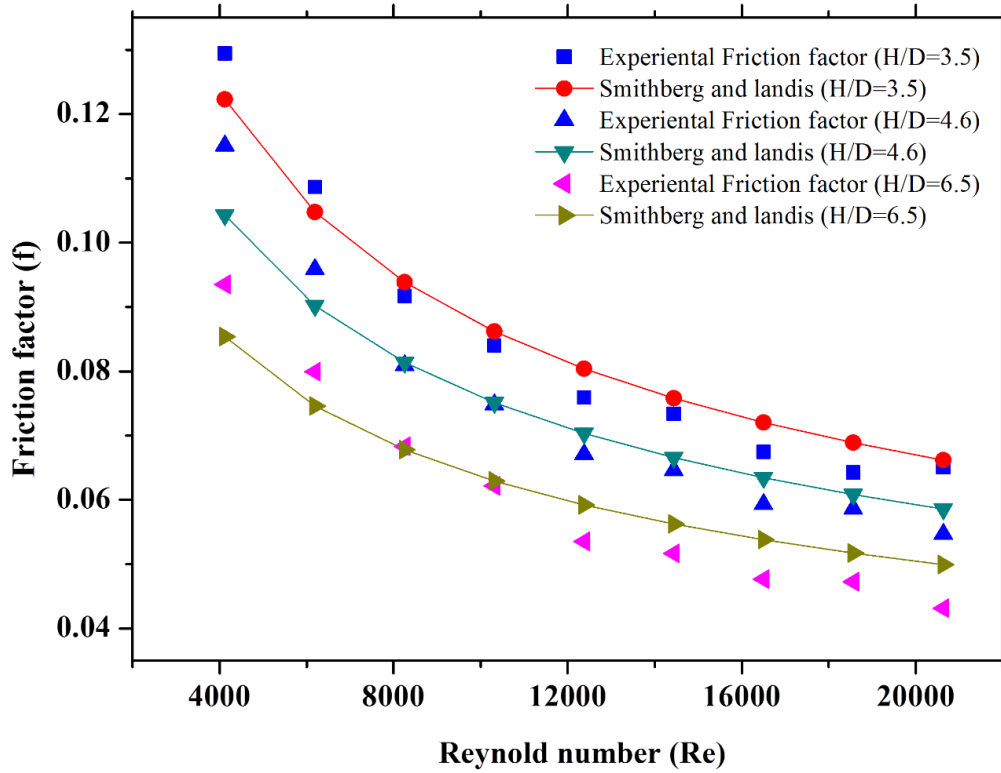


Figure 5.16 (a): comparison of experimental twisted tape with the Smithberg result.

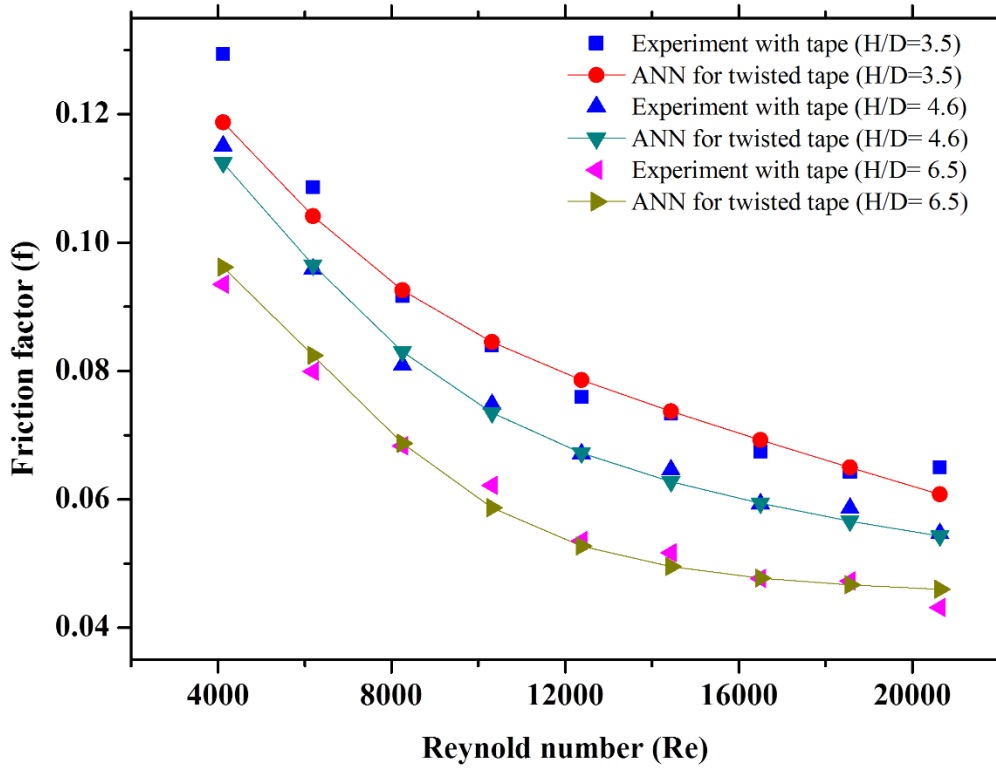


Figure 5.16 (b): Variation of friction factor with the twisted tape ratio.

5.2.4. Plain Tube with TiO₂-water nanofluid

The TiO₂-water nanofluid with different concentration 0.01%, 0.025% and 0.05% were used in plain tube for enhancement the heat transfer coefficient. The friction factor also increases with TiO₂-water nanofluid. Fig 5.17 shows the effect of different concentration of TiO₂-water nanofluid on the friction factor. It was found that with increase in TiO₂ concentration the friction factor increases. The friction factor increases 1%, 1.5% for 0.025%, 0.05% TiO₂-water concentration respectively, as compared to plain tube. The friction factor increases with increase in the TiO₂-water concentration, this is due to increase in the viscosity of fluid and forces exerted by the nanoparticle to the tube wall increases.

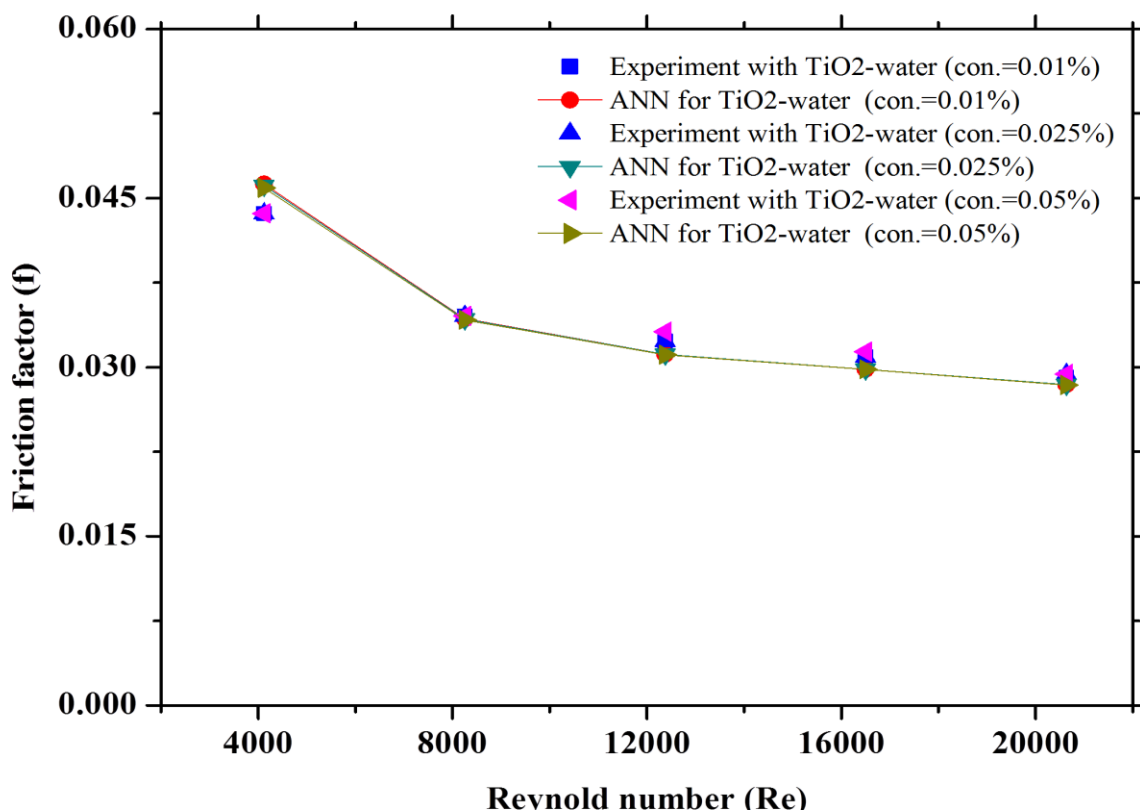


Figure 5.17: Variation of friction factor with the TiO₂ concentration.

5.2.5 Effect of TiO₂-water nanofluid with the Twisted Tape on the friction factor

The TiO₂-water nanofluid concentration 0.025% and with twisted tape ratio 3.5, 4.6 and 6.5 insert were used to study the effect on friction factor. It was found that using nanofluid concentration 0.01% with twisted tape ratio 3.5, friction factor increased 1.96 times as compared to plain tube with water at same operating condition. Furthermore the friction factor increases about 1.63 times for twisted tape ratio 4.6 and 1.14 times for twisted tape

ratio 6.5 as compared to plain tube with water. The friction factor decreases with increase in the Reynold number (Fig 5.18). From Fig.5.18 it is clear that with decrease in the twisted tape ratio there is an enhancement in friction factor at same concentration and operating condition. The reason is that with decrease in the twisted ratio it perturbed to flow. The experimental friction factor value for 0.01% concentration of TiO₂ –water nanofluid with twisted tape ratio (H/D=3.5, 4.6 and 6.5) were compared with artificial neural network and has been shown in Fig. 5.18.

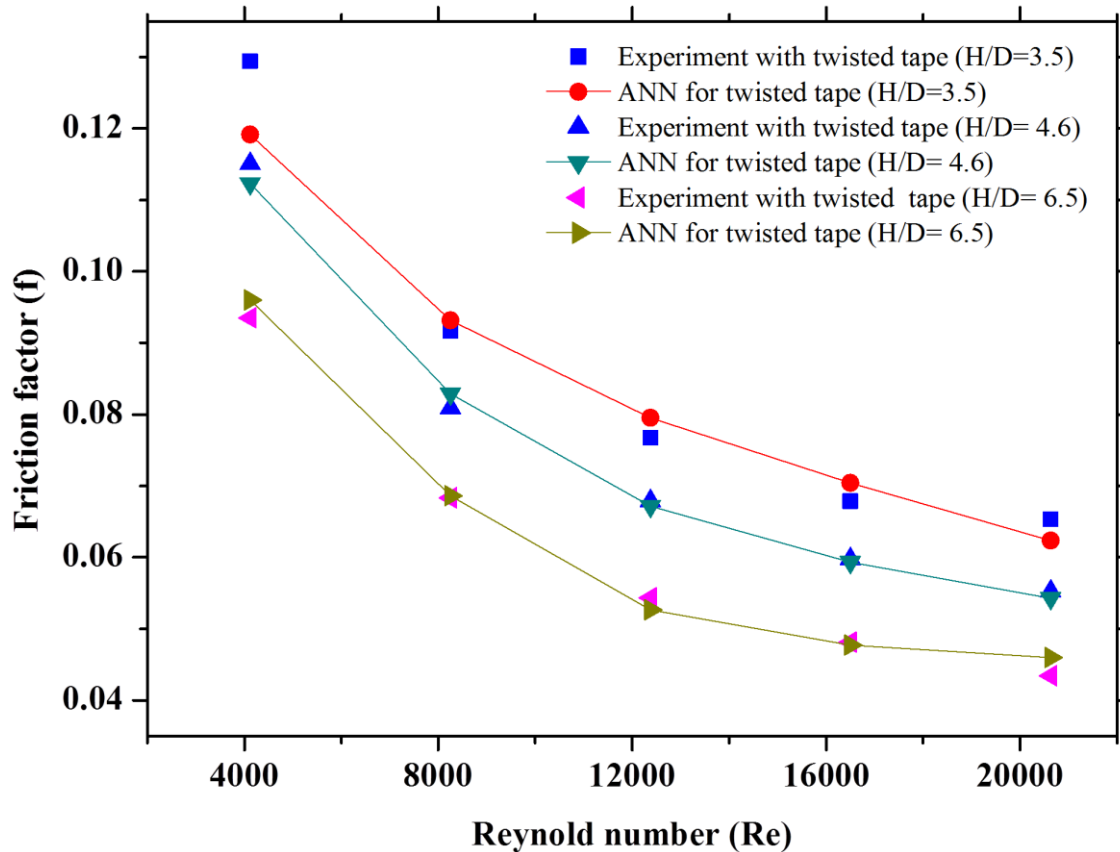


Figure 5.18: Variation of friction factor with the twisted tape ratio (H/D=3.5, 4.6 and 6.5) at 0.01% TiO₂-water concentration

The experimental and ANN predicted friction factor for TiO₂-water nanofluid concentration 0.025% with twisted tape ratio 3.5, 4.6 and 6.5 has been shown in Fig. 5.19. From the Fig 5.19, it is clear that ANN model predicts value of friction factor accurately. It was observed that at same TiO₂-water nanofluid with different twisted tape ratio the friction factor enhances. Friction factor for twisted tape 3.5 with TiO₂-water concentration 0.025% enhances 1.96 times as compared to plain tube with water. The friction factor for same TiO₂-water concentration with 4.6 and 6.5 twisted tape ratio was 1.63 and 1.14 times as compared to water in plain tube.

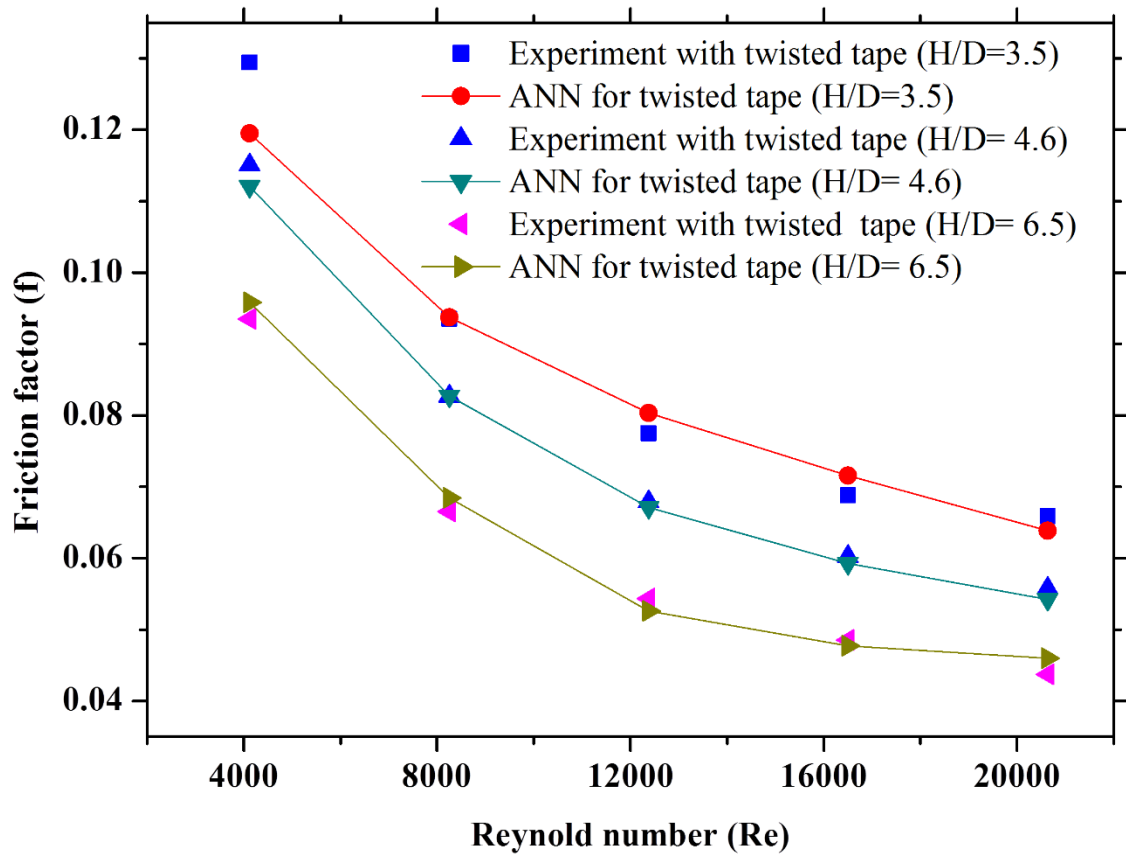


Figure 5.19: Variation of friction factor with the twisted tape ratio (H/D= 3.5, 4.6 and 6.5) at 0.025% TiO₂-water concentration

The effect of TiO₂-water nanofluid 0.05% concentration with twisted tape ratio 3.5, 4.6 and 6.5 on friction factor has been shown in Fig. 5.20. The friction factor is 2.15, 1.63 and 1.14 times higher as compared plain tube with twisted tape ratio 3.5, 4.6 and 6.5 respectively, for 0.05 % TiO₂-water nanofluid. The 0.05% TiO₂-water nanofluid with twisted tape ratio 3.5 shows greater enhancement in friction factor due to fact that the increase in concentration lead to higher viscosity of fluid and twisted tape insert resist the flow in passage. The Fig 5.20 also shows the experimental and ANN predicted friction factor for configuration 3-3-1. The ANN predicts the friction factor with very small deviation as shown in Fig. 5.20.

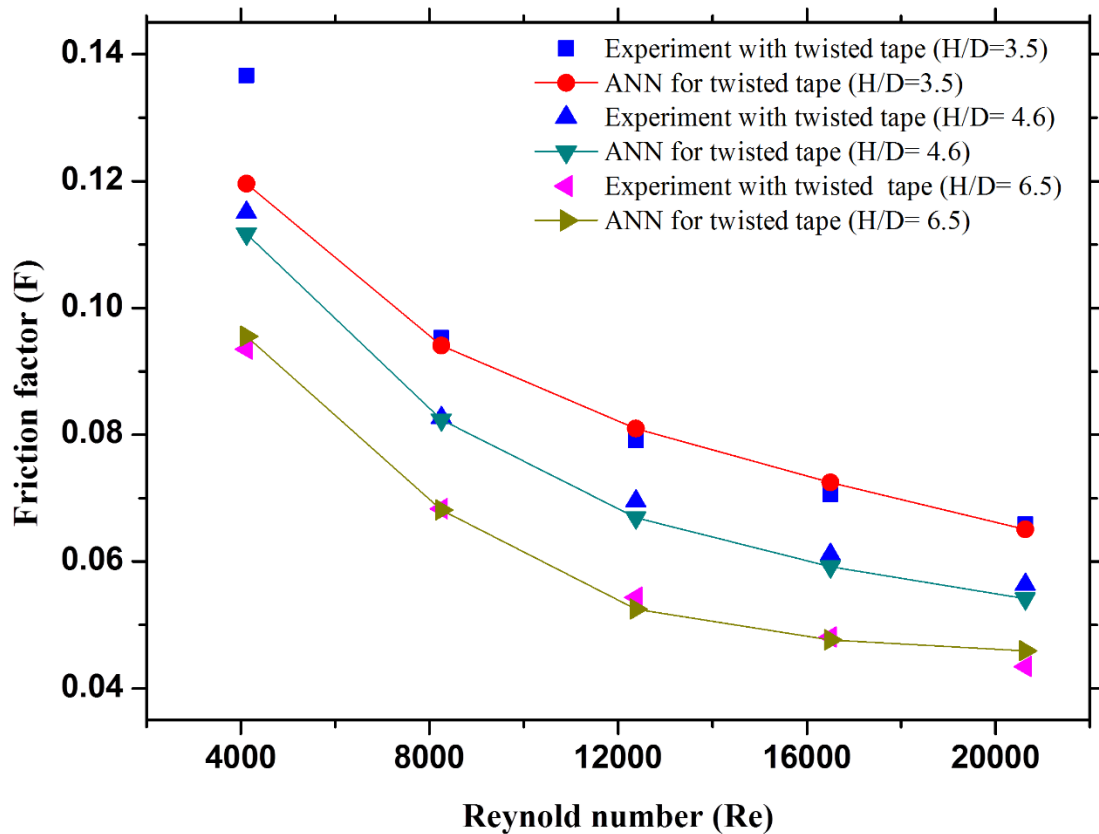


Figure 5.20: Variation of friction factor with the twisted tape ratio (H/D=3.5, 4.6 and 6.5) at 0.05% TiO₂-water concentration

5.2.6 Effect of Plain tube, TiO₂-water nanofluid, Twisted Tape with and without TiO₂-water nanofluid on the friction factor

The TiO₂-water nanofluid with and without twisted tape were used to enhance the heat transfer coefficient, also increased the friction factor. The friction factor decreases with increase in Reynolds number. It was found that by decreasing the twisted tape ratio and increasing the concentration of TiO₂-water lead to increase in friction factor. The comparison of different heat transfer coefficient enhancement technique on the friction factor based has been shown in Fig. 5.21.

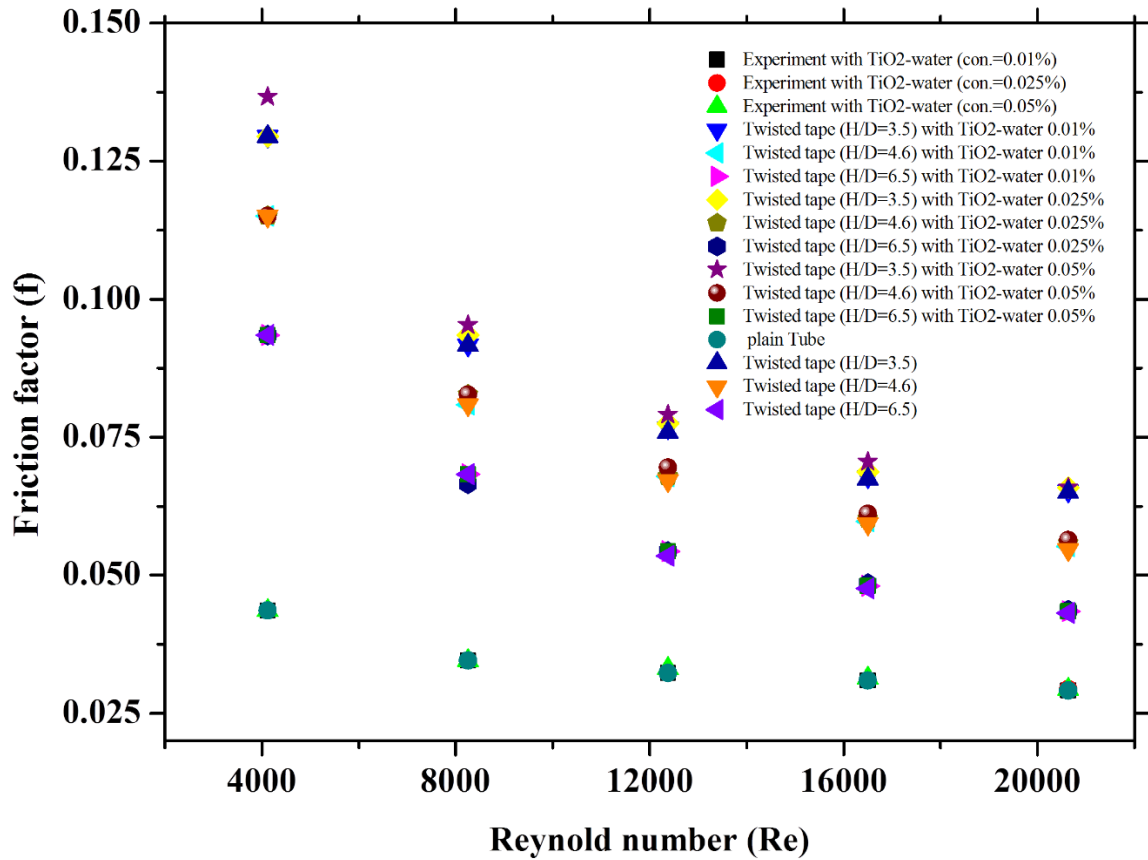


Figure 5.21: Comparison of effect of different heat transfer coefficient enhancement technique on friction factor.

Chapter 6

Conclusion and future Scope

6.1 Conclusion

In the present study the main focus is to investigate the heat transfer coefficient and friction factor of TiO₂-water nanofluid flow through a double tube heat exchanger with twisted tape inserts. The artificial neural network is applied to predict the heat transfer coefficient and friction factor. The following conclusions are drawn:

- The predicted heat transfer coefficient and friction factor with artificial neural network model have good agreement with the experimental data.
- The Nusselt number increases with increase in mass flow rate of hot water.
- The heat transfer coefficient enhanced with decrease in twisted tape ratio as compared to water in a plain tube. The maximum enhanced is 55.4% for twisted tape ratio 3.5 as compared to water.
- The ANN model predicted the heat transfer coefficient for twisted tape more accurately than the Manglik and Bergies correlation.
- By use of TiO₂-water in a plain tube with different concentration the heat transfer coefficient increases. The maximum increase in heat transfer coefficient is 3.2% at 0.05% TiO₂-water nanofluid as compared to water in plain tube.
- Further the enhancement of heat transfer coefficient was observed with twisted tape insert at TiO₂-water different concentration. The maximum enhancement in heat transfer is 59.2% with twisted tape ratio 3.5 and 0.05 % TiO₂-water as compared to base fluid.
- The use of twisted tape increases the heat transfer coefficient but also increase in friction factor. The maximum increase in friction factor is 1.96 with the twisted tape ratio 3.5 as compared to water.
- With increase in the TiO₂-water concentration the friction factor also enhanced. The friction factor increases 1.5% as compared to water.
- The presence of twisted tape with TiO₂-water results in increase in friction factor. The friction factor is increases with the decrease in twisted tape ratio and increase in concentration of TiO₂-water nanofluid.

6.2 Future Scope

- The different type of nanofluid such as TiO_2 , Al_2O_3 and CuO at same concentration will use to conduct the experiment and compare the performance analysis.
- The hybrid nanofluid with twisted tape can checked for better results of heat transfer enhancement.
- The different twisted tape will be used, such as self-rotating, louvered strip and fined twisted tape with same concentration of TiO_2 and performance analysis will compare.
- Empirical correlation for TiO_2 -water with twisted tape can be derived.
- The CFD result can be used to verify the data obtained from experimental result.

References

- Alamgholilou, A. & Esmailzadeh, E. (2012) Experimental investigation on hydrodynamics and heat transfer of fluid flow into channel for cooling of rectangular ribs by passive and EHD active enhancement methods. *Exp. Therm. Fluid Sci.* 38, 61–73.
- Anoop, K. B., Sundararajan, T. & Das, S. K. (2009) Effect of particle size on the convective heat transfer in nanofluid in the developing region. *Int. J. Heat Mass Transf.* 52, 2189–2195.
- Arulprakasajothi, M., Elangovan, K., Reddy, K. H. & Suresh, S. (2015) Heat transfer study of water-based Nanofluids containing TiO₂ nanoparticles. *elsevier*. 2, 3648–3655.
- Azmi, W. H., Sharma, K. V, Mamat, R. & Anuar, S. (2014) Turbulent forced convection heat transfer of nanofluids with twisted tape insert in a plain tube. *Energy Procedia* 52, 296–307.
- Azmi, W. H., Sharma, K. V, Sarma, P. K., Mamat, R. & Anuar, S. (2014) Comparison of convective heat transfer coefficient and friction factor of TiO₂ nano fluid flow in a tube with twisted tape inserts. 81, 84–93.
- Choi, S. U. S. & Eastman, J. A. (1995) Enhancing thermal conductivity of fluids with nanoparticles D.A. Singiner, H.P. Wang , Developments and Application of Non-Newtonian Flows. 66, 99-105.
- Duangthongsuk, W. & Wongwises, S. (2009) Heat transfer enhancement and pressure drop characteristics of TiO₂ – water nanofluid in a double-tube counter flow heat exchanger. *Int. J. Heat Mass Transf.* 52, 2059–2067.
- Eiamsa ard, S., Kiatkittipong, K. & Jedsadaratanachai, W. (2015) Heat transfer enhancement of TiO₂ / water nano fluid in a heat exchanger tube equipped with overlapped dual twisted-tapes. *Eng. Sci. Technol. an Int. J.* 18, 336–350.
- Eiamsa ard, S., Pethkool, S., Thianpong, C. & Promvong, P. (2008) Turbulent flow heat transfer and pressure loss in a double pipe heat exchanger with louvered strip inserts *Int. J. Heat Mass Transf.* 35, 120–129.
- Eiamsa ard, S., Thianpong, C. & Promvong, P. (2006) Experimental investigation of heat transfer and flow friction in a circular tube fitted with regularly spaced twisted tape

- elements *Int. J. Heat Mass Transf.* 33, 1225–1233.
- Elshafei, E. A. M., Mohamed, M. S., Mansour, H. & Sakr, M. (2008) Experimental study of heat transfer in pulsating turbulent flow in a pipe. *Int. J. Heat Fluid Flow* 29, 1029–1038.
- Ermis, K., Erek, A. & Dincer, I. (2007) Heat transfer analysis of phase change process in a finned-tube thermal energy storage system using artificial neural network. *Int. J. Therm. Sci.* 50, 3163–3175.
- Esfe, M. H., Rostamian, H., Afrand, M., Karimipour, A. & Hassani, M. (2015) Modeling and estimation of thermal conductivity of MgO – water / EG (60 : 40) by artificial neural network and correlation . *Int. Commun. Heat Mass Transf.* 68, 98–103.
- Farajollahi, B., Etemad, S. G. & Hojjat, M. (2010) Heat transfer of nanofluids in a shell and tube heat exchanger. *Int. J. Heat Mass Transf.* 53, 12–17.
- Incropera, F.P., DeWitt, P.D., Bergman, T.L. & Lavine, A.S. (2006) Fundamentals of Heat and Mass Transfer, John-Wiley & Sons.
- Godson, L., Deepak, K., Enoch, C., Jefferson, B. & Raja, B. (2013) Heat transfer characteristics of silver / water nano fluids in a shell and tube heat exchanger. *Arch. Civ. Mech. Eng.* 14, 489–496.
- Hasanpour, A., Farhadi, M. & Sedighi, K. (2014) A review study on twisted tape inserts on turbulent flow heat exchangers : The overall enhancement ratio criteria . *Int. Commun. Heat Mass Transf.* 55, 53–62.
- Hojjat, M., Etemad, S. G., Bagheri, R. & Thibault, J. (2011) Thermal conductivity of non-Newtonian nanofluids : Experimental data and modeling using neural network. *Int. J. Heat Mass Transf.* 54, 1017–1023.
- Khedkar, R. S., Sonawane, S. S. & Wasewar, K. L. (2014) Heat transfer study on concentric tube heat exchanger using TiO₂-water based nano fluid. *Int. Commun. Heat Mass Transf.* 57, 163–169.
- Khoshvaght-aliabadi, M. & Eskandari, M. (2015) Influence of twist length variations on thermal-hydraulic specifications of twisted-tape inserts in presence of Cu–water nanofluid. *Exp. Therm. Fluid Sci.* 61, 230–240.

- Lecoeuche, S., Lalot, S. & Desmet, B. (2005) Modelling a non-stationary single tube heat exchanger using multiple coupled local neural networks B. *Int. Commun. Heat Mass Transf.* 32, 913–922.
- Liebenberg, L. & Meyer, J. P. (2007) In-tube passive heat transfer enhancement in the process industry. *Appl. Therm.Eng.* 27, 2713–2726.
- Meybodi, M. K., Naseri, S., Shokrollahi, A. & Daryasafar, A. (2015) Prediction of viscosity of water-based Al₂O₃, TiO₂, SiO₂, and CuO nanofluids using a reliable approach. *Chemometrics and Intelligent Laboratory Systems.* 149, 60–69.
- Naphon, P. (2006) Heat transfer and pressure drop in the horizontal double pipes with and without twisted tape insert. *Int. Commun. Heat Mass Transf.*, 33, 166–175.
- Nazari, M., Ashouri, M., Hasan, M. & Tamayol, A. (2015) International Journal of Thermal Sciences Experimental study of convective heat transfer of a nano fluid through a pipe filled with metal foam. *Int. J. Therm. Sci.* 88, 33–39.
- Peng, H. & Ling, X. (2009) Neural networks analysis of thermal characteristics on plate-fin heat exchangers with limited experimental data. *Appl. Therm. Eng.* 29, 2251–2256.
- Peng, H. & Ling, X. (2008) Optimal design approach for the plate-fin heat exchangers using neural networks cooperated with genetic algorithms. *Appl. Therm. Eng.* 28, 642–650.
- Piriyarungrod, N., Thianpong, C., Pimsarn, M. & Nanan, K. (2015) Heat transfer enhancement by tapered twisted tape inserts. *Elsevier B.V.*
- Prasad, P. V. D., Gupta, A. V. S. S. K. S. & Deepak, K. (2015) Investigation of Trapezoidal-Cut Twisted Tape Insert in a Double Pipe U-Tube Heat Exchanger using Al₂O₃ / Water Nanofluid. *Procedia Mater. Sci.* 10, 50–63.
- Promvongse, P. (2015) Thermal performance in square-duct heat exchanger with quadruple V-finned twisted tapes. *Appl. Therm. Eng.* 91, 298–307.
- Sadeghi, O., Mohammed, H. A., Bakhtiari-nejad, M. & Wahid, M. A. (2016) Heat transfer and nano fluid flow characteristics through a circular tube fitted with helical tape inserts. *Int. Commun. Heat Mass Transf.* 71, 234–244.

- Sajadi, A. R. & Kazemi, M. H. (2011) Investigation of turbulent convective heat transfer and pressure drop of TiO_2 / water nano fluid in circular tube . *Int. Commun. Heat Mass Transf.* 38, 1474–1478.
- Sik, K., Pil, S. & Choi, S. U. S. (2009) Flow and convective heat transfer characteristics of water-based Al_2O_3 nanofluids in fully developed laminar flow regime. *Int. J. Heat Mass Transf.* 52, 193–199.
- Sun, B., Zhang, Z. & Yang, D. (2009) Improved heat transfer and flow resistance achieved with drag reducing Cu nanofluids in the horizontal tube and built-in twisted belt tubes. *Int. J. Heat Mass Transf.* 95, 69–82 (2016).
- Tan, C. K., Ward, J., Wilcox, S. J. & Payne, R. Artificial neural network modelling of the thermal performance of a compact heat exchanger. *Appl. Therm. Eng.* 29, 3609–3617.
- Tian, Z., Gu, B., Yang, L. & Liu, F. (2014) Performance prediction for a parallel flow condenser based on artificial neural network. *Appl. Therm. Eng.* 63.
- Vaferi, B., Samimi, F., Pakgohar, E. & Mowla, D. (2014) Artificial neural network approach for prediction of thermal behavior of nano fluids flowing through circular tubes. *Powder Technol.* 267, 1–10.
- Vasickaninova, A. & Bakosova, Meszaros, A., Klemes J. (2011) Neural network predictive control of a heat exchanger. *Appl. Therm.* 31, 2094–2100.
- Wongcharee, K. & Eiamsa ard, S. (2012) Heat transfer enhancement by using CuO / water nano fluid in corrugated tube equipped with twisted tape Counter arrangement Parallel arrangement Corrugated tube. *Int. Commun. Heat Mass Transf.* 39, 251–257.
- Xie, G. N., Wang, Q. W., Zeng, M. & Luo, L. Q. (2007) Heat transfer analysis for shell-and-tube heat exchangers with experimental data by artificial neural networks approach. *Appl. Therm. Eng.* 27, 1096–1104.
- Yang, Y., Zhang, Z. G., Grulke, E. A., Anderson, W. B. & Wu, G. (2005) Heat transfer properties of nanoparticle-in-fluid dispersions (nanofluids) in laminar flow. *Int.J. Heat Mass transf.* 48, 1107–1116.

- Zamzamian, A., Nasser, S., Doosthoseini, A. & Joneidi, A. (2011) Experimental investigation of forced convective heat transfer coefficient in nanofluids of Al₂O₃ / EG and CuO / EG in a double pipe and plate heat exchangers under turbulent flow. *Exp. Therm. Fluid Sci.* 35, 495–502.
- Zhang, J. & Haghghat, F. (2010) Development of Artificial Neural Network based heat convection algorithm for thermal simulation of large rectangular cross-sectional area Earth-to-Air Heat Exchangers. *Energy Build.* 42, 435–440.

Appendix

Sample Calculation

A.1.1 Nanofluid thermos-physical properties calculation

A.1.1.1 Density of TiO₂-water nanofluid

$$\rho_{nf} = (1 - \Phi)\rho_w + \Phi\rho_{np}$$

For 0.01% concentration

$$\rho_{nf} = 0.01/100(4230) + (1 - 0.01/100)(979.4)$$

$$\rho_{nf} = 979.73 \text{ kg/m}^3$$

Similarly, for 0.025% and 0.05% concentration

$$\rho_{nf0.025} = 980.212 \text{ kg/m}^3$$

$$\rho_{nf0.05} = 981.27 \text{ kg/m}^3$$

A.1.1.2 Specific heat of TiO₂-water nanofluid

The specific heat is calculated by using Xuan and Roetzel correlation

$$C_{p,nf} = \Phi C_{p,np} + (1 - \Phi)C_{p,w}$$

For concentration 0.01%

$$C_p = 0.01/100 \times 683 + (1 - 0.01/100)4188$$

$$C_p = 4183.88 \text{ J/Kg K}$$

Similarly for 0.02% and 0.05% concentration

$$C_{p0.025} = 4187.12 \text{ J/Kg K}$$

$$C_{p0.05} = 4186.24 \text{ J/Kg K}$$

A.1.1.3 Thermal conductivity of TiO₂-water nanofluid

Sharma et al. develop equation for estimating the Thermal conductivity

Equation validation

$$\Phi \leq 4\%, T_{nf} \leq 70^\circ\text{C} \text{ and } d_p \leq 170\text{nm}$$

$$K_r = K_{nf}/K_w = 0.8938 \left(1 + \frac{\Phi}{100}\right)^{1.37} (1 + T_{nf}/70)^{.277} (1 + d_p/150)^{-.0336} (\alpha_p/\alpha_w)^{0.173}$$

$$K_{0.01} = 0.8938(1+.01/100)^{1.37} (1+65/70)^{.2777} \times (1+30/150)^{-.0336} (2.05 \times 10^{-6}/1.61 \times 10^{-4})^{0.01737}$$

$$K_{0.01} = 0.988 \text{ W/mK}$$

Similarly for 0.02% and 0.05% concentration

$$K_{0.025} = 0.989 \text{ W/mK}$$

$$K_{0.05} = 0.989 \text{ W/mK}$$

A.1.1.4 Viscosity of TiO₂-water nanofluid

Sharma et al. develop equation for estimating the viscosity

Equation validation

$$\Phi \leq 4\%, T_{nf} \leq 70^\circ\text{C} \text{ and } d_p \leq 170\text{nm}$$

$$\mu_r = \mu_{nf}/\mu_w = \left(1 + \frac{\Phi}{100}\right)^{11.3} (1 + T_{nf}/70)^{-.038} (1 + d_p/170)^{-.061}$$

$$\mu_{0.01} = (1+.01/100)^{11.3} (1+65/70)^{-.038} (1+30/170)^{-.061}$$

$$\mu_{0.01} = .9653 \text{ kg/m.s}$$

Similarly for 0.02% and 0.05% concentration

$$\mu_{0.025} = .971 \text{ kg/m.s}$$

$$\mu_{0.05} = .9879 \text{ kg/m.s}$$

A.1.2 Heat transfer coefficient calculation

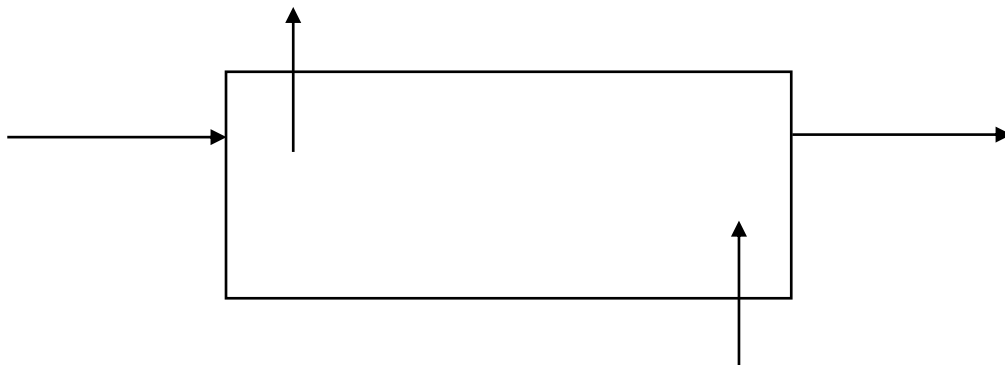


Figure 5.1 counter flow double tube heat exchanger

A.1.2.1 Plain Tube

Heat transfer rate of hot side

$$Q_h = m_h c_{p,w} (T_{h,in} - T_{h,out})$$

$$= 0.0163 \times 4186 (65.6 - 53.4)$$

$$Q_{hot} = 823.4 \text{ W}$$

$$Q_c = m_c c_p (T_{c,out} - T_{c,in})$$

$$= 0.065 \times 4186 (30.2 - 25.4)$$

$$Q_{cold} = 1310 \text{ W}$$

$$Q_{avg} = \frac{Q_c + Q_h}{2}$$

$$Q_{avg} = 1066 \text{ W}$$

$$LMTD = (T_{hi} - T_{co}) - (T_{ho} - T_{ci}) / \ln [(T_{hi} - T_{co}) / (T_{ho} - T_{ci})]$$

$$= (65.6 - 30.2) - (53.4 - 25.4) / \ln [(65.6 - 30.2) / (53.8 - 25.6)]$$

$$LMTD = 31.55^\circ \text{C}$$

$$A_i = \pi d_i l$$

$$= 3.14 \times 0.012 \times 1.5$$

$$= 0.05654 \text{ m}^2$$

$$Q_{avg} = U A_i \Delta T_{LMTD}$$

$$U_i = 1066 / (0.0565 \times 31.55)$$

$$U_i = 598.0 \text{ W/m}^2 \text{C}$$

$$\frac{1}{U_i} = \frac{1}{h_o} + \frac{1}{h_i}$$

$$N_U = \frac{h_o D_h}{K} = 0.023 \text{Re}^{0.8} \text{Pr}^{0.3}$$

$$D_h = D_o - D_i$$

$$= 0.0252 - 0.012 = 0.0132 \text{ m}$$

$$N_{uo} = 0.023 (2650.08)^{0.8} (5.83)^{0.3}$$

$$N_{uo} = 21.38$$

$$N_{uo} = D_h / k$$

$$21.38 = h_o \times 0.0132 / 0.613$$

$$h_o = 992.8 \text{ W/m}^2 \text{C}$$

$$\frac{1}{U_i} = \frac{1}{h_o} + \frac{1}{h_i}$$

$$1/598 = 1/h_i + 1/992.8$$

$$h_i = 1503.7 \text{ W/m}^2\text{C}$$

$$\text{Nu} = 1503.7 \times 0.012 / 0.653$$

$$\text{Nu} = 27.6$$

A.1.2.2 Calibration of plain tube

Dittus Boelter

$$\text{Nu} = \text{Re}^{0.8} \text{Pr}^{0.4}$$

$$= 0.023(4126)^{0.8}(2.66)^{0.4}$$

$$\text{Nu} = 26.55$$

$$\text{Deviation in \%} = (27.6 - 26.55 / 26.55) \times 100 = 4.0\%$$

A.1.2.3 Calibration of twisted tape with Manglik and Bergles

For twisted tape ratio 6.5

Manglik and Bergles equation

$$\text{Nu} = 0.023 \text{Re}^{0.8} \text{Pr}^{0.4} [1 + 0.769 (D/H)] \phi$$

$$\phi = [\pi / (\pi - 4\delta/D)]^{0.8} [(\pi + 2 - 2\delta/D) / (\pi - 4\delta/D)]^{0.2}$$

$$\text{Nu} = 40.27$$

Nusselt number experimentally

Heat transfer rate of hot side

$$Q_h = m_h c_{p,w} (T_{h,in} - T_{h,out})$$

$$= 0.016280 \times 4184 (64.6 - 49.3)$$

$$Q_{hot} = 1004.16 \text{ W}$$

$$Q_c = m_c c_p (T_{c,out} - T_{c,in})$$

$$= 0.0666 \times 4178 (29.1 - 25)$$

$$Q_{cold} = 1130 \text{ W}$$

$$Q_{avg} = (Q_{hot} + Q_{cold}) / 2$$

$$Q_{avg} = 1067.08 \text{ W}$$

$$\text{LMTD} = (T_{hi} - T_{co}) - (T_{ho} - T_{ci}) / \ln [(T_{hi} - T_{co}) / (T_{ho} - T_{ci})]$$

$$= (64.6 - 29.1) - (49.3 - 25) / \ln [(64.6 - 29.1) / (49.3 - 25)]$$

$$\text{LMTD} = 30.69^\circ\text{C}$$

$$A_i = \pi d_i l$$

$$=3.14 \times 0.012 \times 1.5$$

$$=0.05654 \text{ m}^2$$

$$Q_{\text{avg}} = UA_i \Delta T_{\text{LMTD}}$$

$$U_i = 1083 / (0.0565 \times 30.69)$$

$$U_i = 624 \text{ W/m}^2\text{C}$$

$$\frac{1}{U_i} = \frac{1}{h_o} + \frac{1}{h_i}$$

$$N_U = \frac{h_o D_h}{K} = 0.023 \text{Re}^{0.8} \text{Pr}^{0.3}$$

$$D_h = D_o - D_i$$

$$=0.0252 - 0.012 = 0.0132 \text{ m}$$

$$N_{u_o} = 0.023(2650.08)^{0.8}(5.83)^{0.3}$$

$$N_{u_o} = 21.38$$

$$N_{u_o} = h_o D_h / k$$

$$21.38 = h_o \times 0.0132 / 0.613$$

$$h_o = 992 \text{ W/m}^2\text{C}$$

$$1/U_i = 1/h_i + 1/h_o$$

$$1/648.5 = 1/h_i + 1/992$$

$$h_i = 1869 \text{ W/m}^2\text{C}$$

$$Nu = 1869 \times 0.012 / 0.653$$

$$Nu = 34.46$$

Deviation of Nusselt number predicted by the Manglik and Bergies

$$\text{Deviation in \%} = (34.46 - 36.4 / 36.4) \times 100 = 5.4\%$$

A.1.3 Friction factor calculation

A.1.3.1 Plain Tube

Darcy equation is used to determine the friction factor

$$F = 2D\Delta P / \rho V^2 L$$

$$F = 0.0436$$

A.1.3.2 Calibration of plain tube with Blasius equation

$$F = 0.318 / \text{Re}^{0.25}$$

$$F = 0.318 / 4294.6^{0.25}$$

$F=0.0396$

Deviation of experimental friction factor from the predicted friction factor by Blasius equation

Deviation in % = $(0.0436-0.0396/.0396) \times 100=10.1\%$